AD-A146 414 NAVSTAR GPS (GLOBAL POSITIONING SYSTEM) MARINE RECEIVER 1/1
PERFORMANCE ANALYSIS(U) TRANSPORTATION SYSTEMS CENTER
CAMBRIDGE MA J C PREISIG SEP 84 DOT-TSC-CG-83-6

UNCLASSIFIED USCG-D-25-84 F/G 17/7 NL

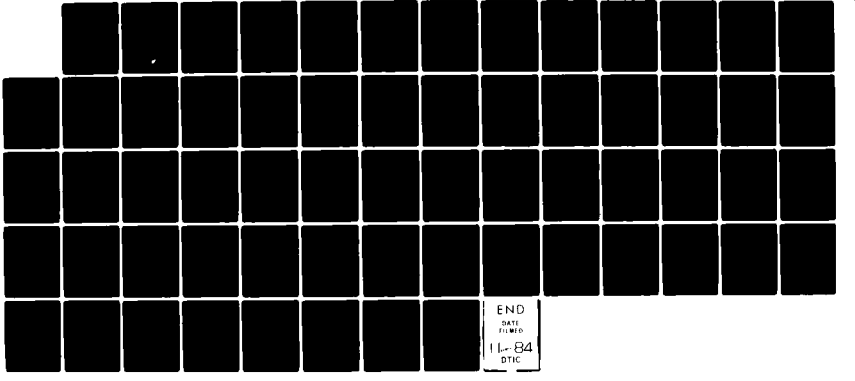

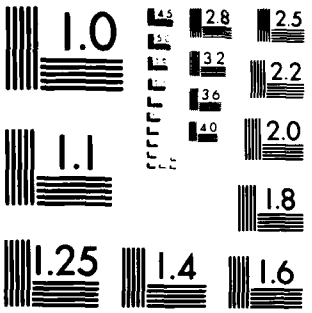

(12)

CG-D-25-84
DOT-TSC-CG-83-6

NAVSTAR GPS Marine Receiver Performance Analysis

LTJG J.C. Preisig

Transportation Systems Center
Cambridge MA 02142

September 1984
Final Report

U.S. Department of Transportation
United States Coast Guard

Office of Research and Development
Navigation Systems Technology Branch
Washington DC 20593

Technical Report Documentation Page

1. Report No.	2. Government Accession No.	3. Recipient's Catalog No.
CG-D-25-84	AD-A146 414	

4. Title and Subtitle
NAVSTAR GPS MARINE RECEIVER PERFORMANCE ANALYSIS

5. Report Date
September 1984

6. Performing Organization Code
DTS-53

7. Author(s)
LTJG J.C. Preisig

8. Performing Organization Report No.
DOT-TSC-CG-83-6

9. Performing Organization Name and Address
U.S. Department of Transportation
Research and Special Programs Administration
Transportation Systems Center
Cambridge MA 02142

10. Work Unit No. (TRAIS)
CG445/R4010

11. Contract or Grant No.

12. Sponsoring Agency Name and Address
U.S. Department of Transportation
United States Coast Guard
Office of Research and Development
Washington DC 20593

13. Type of Report and Period Covered
Final Report
Aug 1982 to Dec 1983

14. Sponsoring Agency Code
G-DST-1

15. Supplementary Notes

16. Abstract

This report is an analysis and comparison of the capability of several NAVSTAR GPS receiver configurations to provide accurate position data to the civil marine user. The NAVSTAR GPS system itself has the potential to provide civil marine users with a position fixing capability having an accuracy, coverage, and availability previously unattainable from any single system. This study utilizes theoretical design formulas and a Monte Carlo type navigation processor simulation program, and discusses various performance tradeoffs.

17. Key Words	18. Distribution Statement
Global Positioning System (GPS), Alpha/Beta Tracker, Receiver Module, Navigation Processor Module, Kalman Filter	DOCUMENT IS AVAILABLE TO THE PUBLIC THROUGH THE NATIONAL TECHNICAL INFORMATION SERVICE, SPRINGFIELD, VIRGINIA 22161

19. Security Classif. (of this report)	20. Security Classif. (of this page)	21. No. of Pages	22. Price
Unclassified	Unclassified	70	

Form DOT F 1700.7 (8-72) Reproduction of completed page authorized

PREFACE

The work described in this report was performed in support of the Office of Research and Development of the United States Coast Guard. The Coast Guard has the major responsibility in developing the Department of Transportation's position on the civil radionavigation systems mix for marine navigation. This effort supports that responsibility.

The work was performed at the Transportation Systems Center's Navigation Systems Division. This report is the final report of the results obtained over a period of eighteen months.

The author thanks Dr. Rudolph Kalafus and Dr. John Heurtley for their guidance and support throughout the duration of the project. The efforts of Dr. Norman Knable and Janis Vilcans in providing helpful suggestions are greatly appreciated, as are the efforts of LCDR John Quill of the Office of Research and Development, USCG in providing constructive criticism of this report.

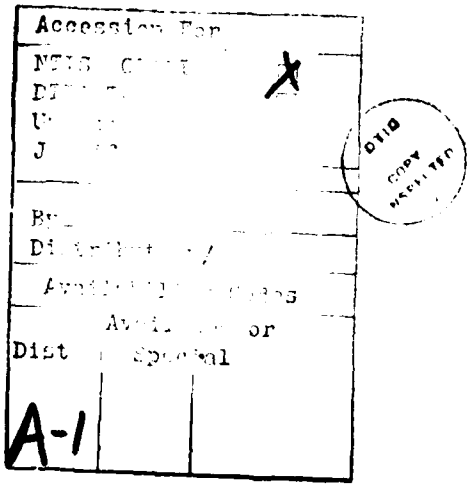

METRIC CONVERSION FACTORS

Approximate Conversions to Metric Measures

Symbol	When You Know	Multiply by	To Find	Symbol
		LENGTH		
in	inches	2.5	centimeters	cm
ft	feet	30	centimeters	cm
yd	yards	0.9	meters	m
mi	miles	1.6	kilometers	km
		AREA		
in^2	square inches	6.5	square centimeters	cm^2
ft^2	square feet	0.09	square meters	m^2
yd^2	square yards	0.8	square meters	m^2
mi^2	square miles	2.6	square kilometers	km^2
	acres	0.4	hectares	ha
		MASS (weight)		
oz	ounces	28	grams	g
lb	pounds	0.45	kilograms	kg
	short tons (2000 lb)	0.9	tonnes	t
		VOLUME		
tsp	teaspoons	5	milliliters	ml
Tbsp	tablespoons	15	milliliters	ml
fl oz	fluid ounces	30	milliliters	ml
c	cups	0.24	liters	l
pt	pints	0.47	liters	l
qt	quarts	0.95	liters	l
gal	gallons	3.8	liters	l
ft^3	cubic feet	0.03	cubic meters	m^3
yd^3	cubic yards	0.76	cubic meters	m^3
		TEMPERATURE (exact)		
°F	Fahrenheit temperature	5/9 (after subtracting 32)	Celsius temperature	°C

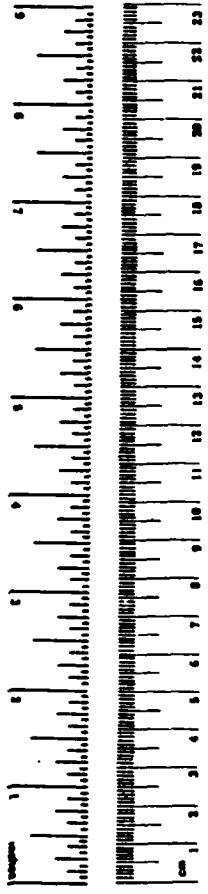

Approximate Conversions from Metric Measures

Symbol	When You Know	Multiply by	To Find	Symbol
		LENGTH		
mm	millimeters	0.04	inches	in
cm	centimeters	0.4	inches	in
m	meters	3.3	feet	ft
m	meters	1.1	yards	yd
km	kilometers	0.6	miles	mi
		AREA		
cm^2	square centimeters	0.16	square inches	in^2
m^2	square meters	1.2	square yards	yd^2
km^2	square kilometers	0.4	square miles	mi^2
ha	hectares (10,000 m^2)	2.5	acres	
		MASS (weight)		
g	grams	0.035	ounces	oz
kg	kilograms	2.2	pounds	lb
t	tonnes (1000 kg)	1.1	short tons	
		VOLUME		
ml	milliliters	0.03	fluid ounces	fl oz
l	liters	2.1	pints	pt
l	liters	1.06	quarts	qt
l	liters	0.26	gallons	gal
m^3	cubic meters	35	cubic feet	ft^3
m^3	cubic meters	1.3	cubic yards	yd^3
		TEMPERATURE (exact)		
°C	Celsius temperature	9/5 (then add 32)	Fahrenheit temperature	°F

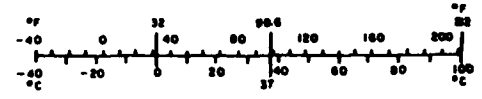

TABLE OF CONTENTS

LIST OF FIGURES

LIST OF TABLES

1. INTRODUCTION

1.1 OBJECTIVE

The NAVSTAR GPS system has the potential to provide civil marine users with a position fixing capability with an accuracy, coverage, and availability previously unattainable from any single system. The position data accuracy which is achievable using the system's Coarse/Acquisition (C/A) signal will heavily influence the usefulness of the system to the civil marine user. To a great extent this achievable accuracy will depend on the specific design characteristics of the user's receiver. The objective of this study is to analyze and compare the capability of several NAVSTAR GPS receiver configurations to provide accurate position data to the civil marine user.

1.2 SCOPE

A complete NAVSTAR GPS receiver can be divided into two major modules: the receiver module and the navigation processor module (Figure 1-1).

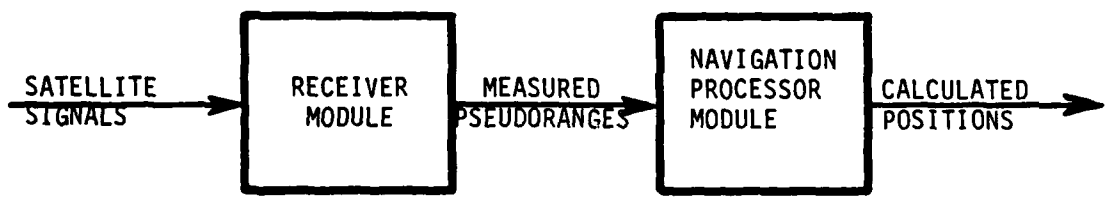

FIGURE 1-1. GPS RECEIVER BLOCK DIAGRAM

The receiver module acquires and tracks the signals being transmitted by selected satellites and measures the pseudorange to each satellite being tracked. Using the pseudorange measured by the receiver module, the navigation processor module estimates the user's position.

An investigation of performance tradeoffs in selecting the receiver module parameters was performed by Mr. James Kuhn and is presented in Appendix A of Reference 3. This work was continued by the author and a summary of the combined results is contained in Appendix A of this report.

Sections 2 and 3 of this report cover the investigation of performance tradeoffs in selecting various navigation processor module configurations and parameters. The criteria by which the navigation processor module's performance is measured is the horizontal accuracy of its position output. The Federal Radionavigation Plan's H/HE navigation requirement of a maximum 2 drms error ranging from 8 to 20 meters is used as a standard for comparison purposes. Section 2 consists of an analysis of several navigation module configurations, and Section 3 presents the results of computed simulations of the operation of the navigation modules. The study has been carried out utilizing primarily theoretical design formulas and a Monte Carlo type navigation processor simulation program. A description of the simulation program is contained in Appendix C.

Section 2.1 presents a description and mathematical analysis of a navigation processor consisting of a position calculation algorithm and an alpha/beta tracker. The tracker is considered in both its standard and switched configurations. The position calculation algorithm utilizes a three-satellite solution and is described in detail in Appendix B. Section 2.2 presents a description and analysis of a navigation processor consisting of a Kalman filter. This section draws heavily upon the concepts developed in the alpha/beta tracker analysis in Section 2.1. Section 2.3 presents a discussion of two types of position errors which are of special concern when using the navigation processor configurations discussed in this report. The first type of error is the transient position error, which develops when the receiver switches from one satellite constellation to another. The second type of error is the position bias error, which results from an incorrect estimation of the user's altitude when only three satellites are being used in determining the user's position.

Section 3 presents the results of the navigation processor simulator described earlier. The simulation is run using all of the navigation processor configurations described in Section 2. The simulation is also run with an incorrect assumption for the user's altitude and with large satellite switching transients.

Section 4 presents conclusions based upon the results presented in Section 3.

2. NAVIGATION PROCESSOR MODULE

The function of the navigation processor is to transform the pseudorange measurements supplied by the receiver module into user position estimates. There are two primary methods of accomplishing this transformation.

The first method utilizes an algorithm (Appendix B) to transform a set of pseudorange measurements into an unfiltered (noisy) position estimate and then utilizes an alpha/beta tracker to reduce the noise error present in the position estimates (Figure 2-1). The second method utilizes a Kalman filter to make a single transformation from a set of pseudorange measurements to a filtered user postion estimate (Figure 2-2).

The above methods can be implemented on a receiver which tracks three active satellites and utilizes an estimate of the user's altitude, or on a receiver which tracks four or more satellites. The algorithm in Appendix B utilizes a three-satellite position calculation.

2.1 THE ALPHA/BETA TRACKER

The first method of transforming pseudorange measurements into an estimated user position utilizes a position calculation algorithm and an alpha/beta tracker. The discussion here will focus on the operation of the alpha/beta tracker. The implementation of the position calculation (Appendix B) is discussed briefly in Section 2.3.

The satellite signals being monitored by the receiver module are contaminated by noise. It is assumed that this noise is white with a zero mean and a Gaussian amplitude distribution. This noise results in a noise error in the pseudorange measurements which leads to a noise error in the unfiltered position data. The purpose of the alpha/beta tracker is to filter as much of this noise as possible out of the position data.

The alpha/beta tracker filters position estimates which it receives from the position calculator at the end of each update period. These update periods (T_{up}) are of the same length as the receiver module update periods discussed in Appendix A. The position estimates are assumed to be in earth-centered, earth-fixed Cartesian

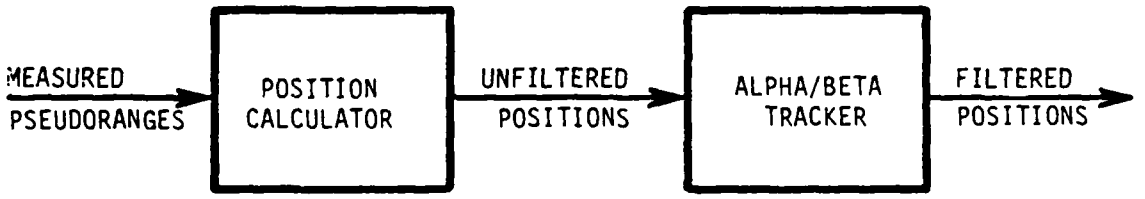

FIGURE 2-1. NAVIGATION PROCESSOR MODULE WITH ALPHA/BETA TRACKER

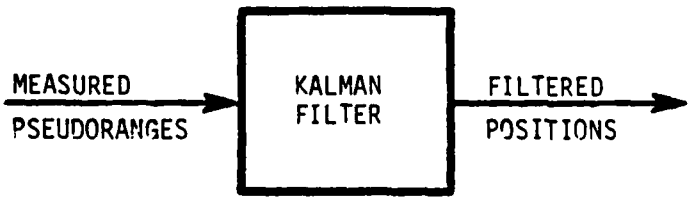

FIGURE 2-2. NAVIGATION PROCESSOR MODULE WITH KALMAN FILTER

coordinates; and separate alpha/beta trackers are used to independently filter each of the three position variables X, Y, and Z. The following description of alpha/beta tracker operation describes a single tracker filtering a single position variable. In this case, the X variable is used. Separate trackers would be used to independently filter the Y and Z variables.

2.1.1 Alpha/Beta Tracker Operation

At the end of the k^{th} update period, the tracker receives an unfiltered position estimate (X_k) from the position calculator. The tracker compares this unfiltered position with the predicted position ($\hat{X}_k$), which the tracker had predicted as the user's position at the end of the k^{th} update period. The tracker then calculates the filtered position ($\bar{X}_k$), which is a weighted average of the predicted position and unfiltered measured position, as in the relation

$$\bar{X}_k = (1 - \alpha)\hat{X}_k + \alpha X_k \qquad \text{Eq. (1)}$$

Equation (1) is the mathematical relationship between filtered position, unfiltered position, and predicted position. The weighting parameter, alpha, is allowed to vary between zero and one. If alpha equals zero, the filtered position equals the predicted position. As alpha increases, more weight is placed on the unfiltered measured position and less on the predicted position. If alpha equals one, the filtered position equals the unfiltered measured position.

The tracker next computes a filtered estimate of the user's velocity ($\bar{\dot{X}}_k$). The tracker first computes the unfiltered measured velocity ($\dot{X}_k$) of the user as in the relation

$$\dot{X}_k = (\bar{X}_k - \bar{X}_{(k-1)})/T_{up} \qquad \text{Eq. (2)}$$

The tracker then takes a weighted average of the predicted and unfiltered measured velocity to compute the filtered velocity estimation (X) via the equation

$$\bar{\dot{X}}_k = (1 - \beta)\hat{\dot{X}}_k + \beta \dot{X}_k. \qquad \text{Eq. (3)}$$

The tracker then predicts the user's future velocity and position using its filtered estimates of the user's current velocity and position and a second order model of user motion. The use of a second order model for user motion means that the tracker assumes a constant user velocity (zero acceleration). Therefore, the tracker sets the predicted future velocity equal to the current filtered velocity

$$\hat{\dot{X}}_{(k+1)} = \bar{\dot{X}}_k. \qquad \text{Eq. (4)}$$

The tracker predicts the user's position

$$\hat{X}_{(k+1)} = \bar{X}_k + T_{up}\,\bar{\dot{X}}_k. \qquad \text{Eq. (5)}$$

The tracker is then ready to accept another unfiltered measured position.

Equations (1) through (5) can be combined and simplified to yield the following three equations, which are the ones most often used to implement the alpha/beta tracker:

$$\bar{X}_k = \hat{X}_k + \alpha(X_k - \hat{X}_k) \qquad \text{Eq. (6)}$$

$$\bar{\dot{X}}_k = \bar{\dot{X}}_{(k-1)} + \beta/T_{up}\,(X_k - \hat{X}_k), \qquad \text{Eq. (7)}$$

$$\hat{X}_{(k+1)} = \bar{X}_k + T_{up}\,\bar{\dot{X}}_k. \qquad \text{Eq. (8)}$$

The filter parameters alpha and beta can be varied independently. However, the relative magnitude of alpha and beta determines the amount of damping in the tracker's response. Various relationships between alpha and beta have been developed which "optimize" the tracker's response. One widely accepted relationship was developed by T.R. Benedict and G.W. Bordner (Reference 1). This relationship

$$\beta = \alpha^2/(2-\alpha) \qquad \text{Eq. (9)}$$

yields a slightly underdamped tracker response. This relationship will be assumed to hold true for the duration of this study.

The alpha/beta tracker is a discrete time, unity gain, low pass filter. While the alpha/beta relationship determines the filter damping, the magnitude of alpha and beta determines the filter bandwidth. Reducing alpha and beta reduces the bandwidth, and increasing alpha and beta increases the bandwidth. As alpha and beta vary from zero to one, the bandwidth varies from 0 Hz to $(1/2T_{up})$ Hz. Therefore, the amount of noise in the filtered position data can be reduced by decreasing alpha and beta.

The penalty paid for reducing alpha and beta is in the form of an increased tracker time constant. Because the tracker incorporates a second order model of user motion, an error will be induced in the estimated user position whenever the user undergoes acceleration. The time required to eliminate the error is proportional to the tracker time constant. If the user undergoes constant acceleration, such as during a turn, the tracker estimates of user position will continually be in error. For constant accelerations, the error will be constant and will be proportional to the time constant of the tracker. Therefore, reducing alpha and beta will result in an increase in the acceleration induced bias error in the filtered position data.

In his paper, "Alpha-Beta Tracking Errors for Orbiting Targets" (Reference 2), Sinsky developed expressions for the magnitude of the noise reduction afforded by a tracker and for the magnitude of the acceleration-induced bias error for a user undergoing constant linear acceleration. The former, expressed as the ratio of the variance of the filtered output signal to the variance of the unfiltered input signal, is given by the equation

$$K_{\bar{x}} = \sigma_{\bar{x}}^2/\sigma_x^2 = \frac{2\alpha^2 + \beta(2 - 3\alpha)}{4 - \beta - 2\alpha} \qquad \text{Eq. (10)}$$

where $K_{\bar{x}}$ is the variance reduction ratio. When alpha equals one, $k_{\bar{x}}$ equals one for all values of beta. This is to be expected because when alpha equals one, the filtered position is the same as the unfiltered position and there is no reduction in the noise present in the data. The approximate expression for acceleration induced bias error during constant linear acceleration is

$$|\epsilon_{\bar{x}}| = \frac{(1 - \alpha)}{\beta} \; a \; T_{up}^2 \qquad \text{Eq. (11)}$$

where "a" is the vessel acceleration. When alpha equals one, $|\Sigma_{\bar{x}}|$ equals zero for all non-zero values of beta. As with the variance reduction ratio, this result is expected. When the filtered data equals the unfiltered data, the filter itself cannot contribute any acceleration-induced bias error. It can be shown that this error applies to constant centripetal acceleration in the two-dimensional case. Table 2-1 shows the variance reduction ratio and acceleration-induced bias as a function of alpha for vessel acceleration of 0.13 meters/sec^2 and an update period of 5.4 seconds. The update period and vessel acceleration were chosen as representative values encountered in the marine environment.

TABLE 2-1. VARIANCE REDUCTION RATIO AND ACCELERATION-INDUCED BIAS ERROR VS. ALPHA

ALPHA	.10	.20	.30	.40	.50	.60	.70	.80	.90	1.0
$K_{\bar{x}}$	.08	.15	.24	.32	.41	.51	.61	.71	.84	1.0
$\lvert\epsilon_{\bar{x}}\rvert$(meters)	648	136	50	23	11	5.9	3.0	1.4	.51	0.0

The data in Table 2-1 illustrates the fundamental compromise which must be made when selecting alpha for a tracker. If alpha is small, the variance reduction ratio is small but the acceleration-induced bias error is large. If alpha is large, the acceleration-induced bias error is small but the variance reduction ratio approaches one. The selection of alpha involves balancing these two factors to achieve a satisfactory overall accuracy under specified noise and acceleration conditions. As a measure of overall positioning accuracy, a criterion function ($J_{\bar{x}}$) is defined as equal to the two sigma value of the noise-induced error plus the acceleration-induced error. This is based upon the worst case assumption of the two errors adding constructively. Thus,

$$J_{\bar{x}} = 2\sigma_{\bar{x}} + |\Sigma_{\bar{x}}| . \qquad \text{Eq. (12)}$$

From Equation (10),

$$\sigma_{\bar{x}} = \sigma_x \sqrt{K\bar{x}} \qquad \text{Eq. (13)}$$

where σ_x is the product of the receiver module's code chip error σ_c and the Horizontal Dilution of Position (HDOP); i.e.,

$$\sigma x = \sigma c \bullet (\text{HDOP}) \qquad \text{Eq. (14)}$$

The quantity HDOP is dependent on the geometry of the satellite constellation and is the ratio of the magnitude of the position error to the magnitude of the pseudorange error which caused the position error. The code chip error is discussed in Appendix A and is the steady state noise-limited code chip misalignment error expressed in meters. In this report, pseudorange error can be equated with code chip error. This means that the effects of the other error sources, such as unmodeled changes in the propagation velocity of the satellites' signals through the atmosphere, will be ignored.

If alpha, beta and T_{up} are selected to minimize $J_{\bar{x}}$, there is an acceptable compromise between reducing noise-induced error and reducing acceleration induced error. Figure 2-3 is a plot of $J_{\bar{x}}$ as a function of alpha for various levels of vessel acceleration.

The conditions used in generating Figure 2-3 were T_{up} = 5.4 sec, C/N_o = 37 dB-Hz, B_{IF} = 200 Hz, $\Delta T/T_c$ = 0.5, T_d = 0.01 sec and HDOP = 2. Acceleration ranges from 0 to 0.02 G's. As a reference, a ship traveling at 20 knots and making a turn with a radius of 880 yds and a vessel traveling at 10 knots and making a turn with a radius of 220 yds are both accelerating at 0.0135 G's.

The horizontal dotted line in Figure 2-3 represents the value of the criterion function J_x and corresponds to an unfiltered position output. J_x is computed as

$$J_x = 2\sigma_x. \qquad \text{Eq. (15)}$$

The J_x equals $J_{\bar{x}}$ when alpha equals one. This is to be expected since an alpha/beta tracker with an alpha of one passes the position data though unchanged.

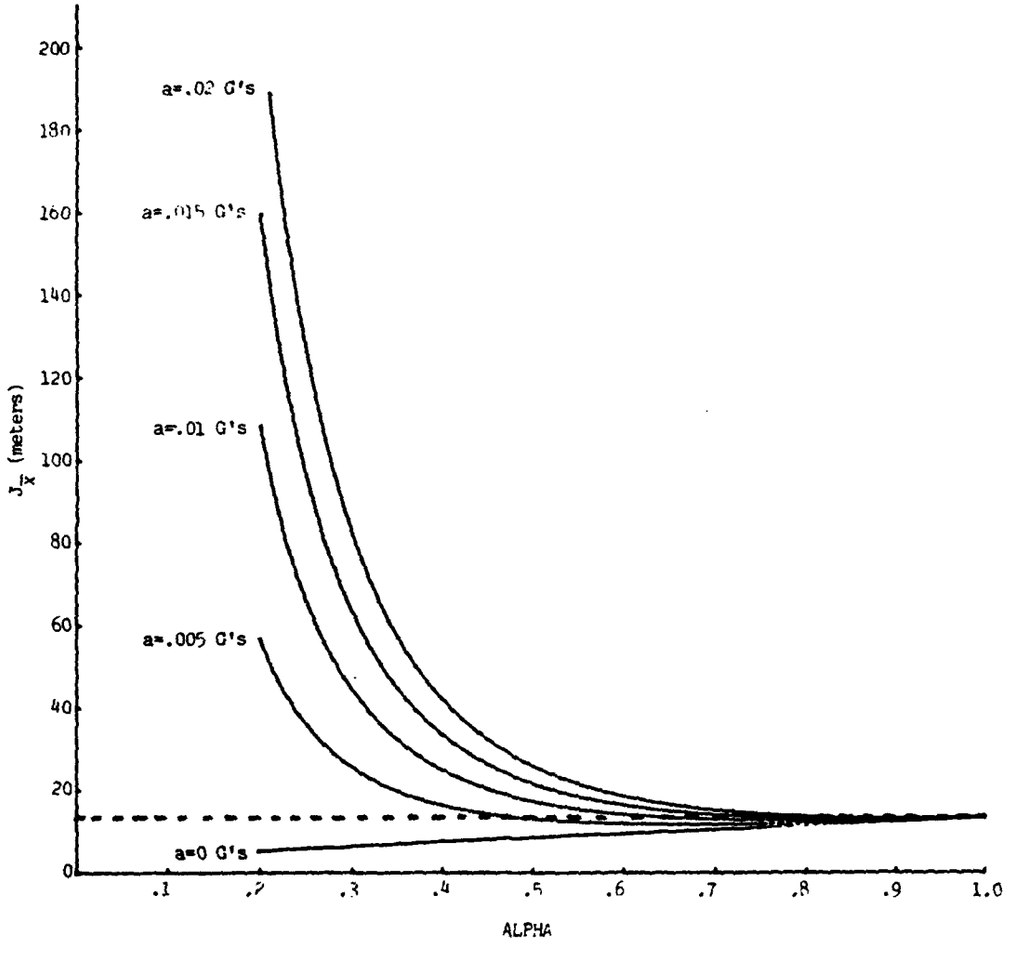

FIGURE 2-3. CRITERION FUNCTION ($J_{\bar{x}}$) VS. ALPHA FOR VARIOUS ACCELERATION CONDITIONS (T_{up} = 5.4 sec)

Figure 2-3 shows that at very low levels of acceleration or large values for alpha the filtered data is more accurate than the unfiltered data. However, when using values which approach one for alpha, there is a corresponding increase in the variance of the filtered position data, as shown in Table 2-1. One way to reduce the magnitude of the position error during periods of acceleration is to decrease the update period. Figure 2-4 contains the same information contained in Figure 2-3 but with the update period reduced to 3 seconds.

When comparing Figures 2-3 and 2-4, it can be seen that when the vessel is undergoing acceleration, the magnitude of the criterion function is greatly reduced when T_{up} is reduced. However, when the vessel is experiencing no acceleration, the magnitude of the criterion function increases when T_{up} is reduced. A more suitable solution to the problem of providing high accuracy during periods of no acceleration without suffering large errors when the user's vessel experiences acceleration is to use a tracker with variable alphas.

2.1.2 The Switched Alpha/Beta Tracker

A switched alpha/beta tracker is one form of a variable alpha tracker. When the tracker senses no vessel acceleration, it displays filtered position data to the user. When the tracker senses vessel acceleration, it displays unfiltered position data to the user. From the user's viewpoint, this is equivelent to varying alpha between some preset value and the value "one" in response to vessel accelerations.

It is important to note that in actual operation the tracker switches between displaying filtered and unfiltered data rather than actually varying its alpha. This is important because the predicted position output of the fixed alpha tracker (alpha less than one) is used in detecting vessel accelerations. This predicted position is subtracted from the unfiltered position as shown in Equation (16),

$$\delta x,k = X_k - \hat{X}_k. \qquad \text{Eq. (16)}$$

If the vessel is not accelerating, the difference ($\delta_{x,k}$) will have a zero mean over time. If the vessel is accelerating, the difference will have a non-zero mean on the order of the magnitude of the acceleration-induced bias error created by the tracker. If the difference is passed through a low pass filter and the output analyzed, vessel

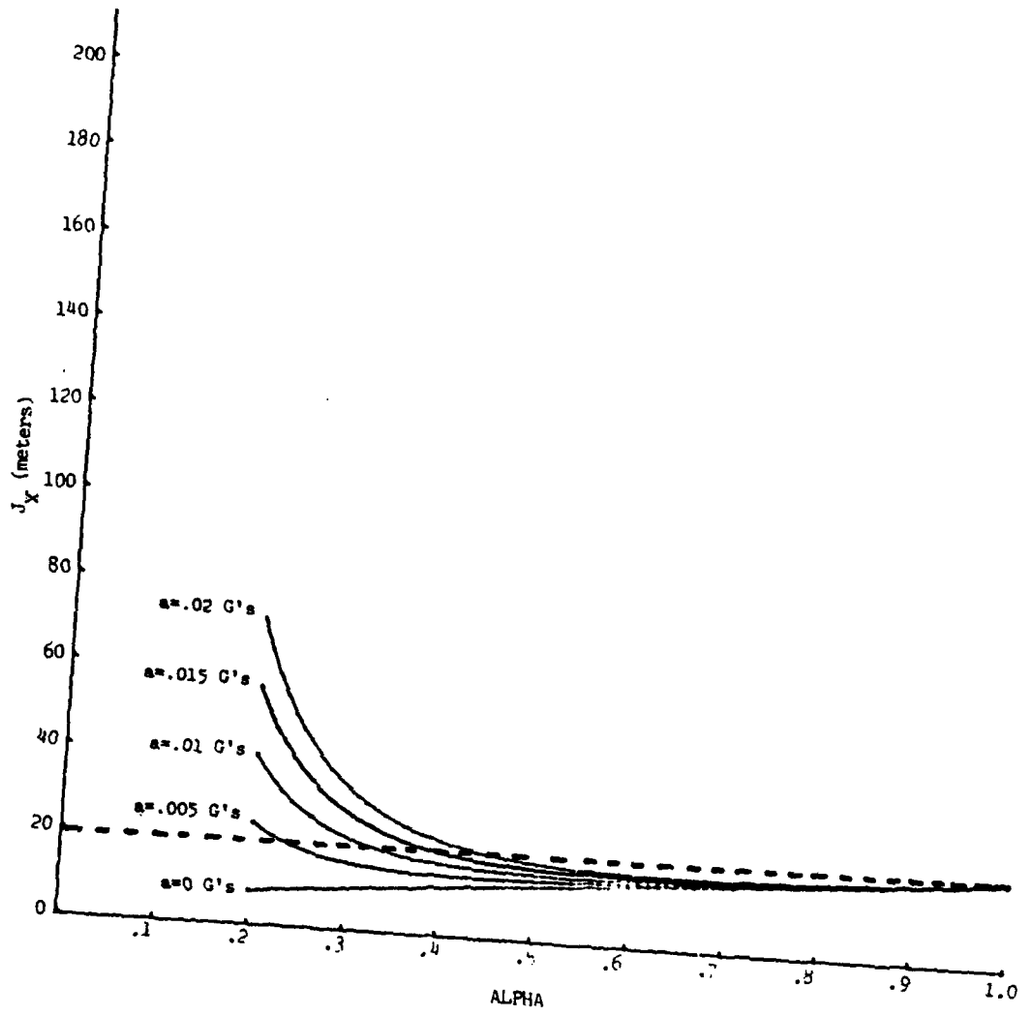

FIGURE 2-4. CRITERION FUNCTION (J_x) VS. ALPHA FOR VARIOUS ACCELERATION CONDITIONS (T_{up} = 3.0 sec)

accelerations can be reliably detected. Using an approach analogous to the alpha/beta tracker, a filtered position difference $\bar{\delta}_{x,k}$ can be developed as

$$\bar{\delta}x,k = (1 - \Gamma)\,\delta_{x,k-1} + \Gamma\,\delta_{x,k}. \qquad \text{Eq. (17)}$$

Here Γ is the low-pass filter constant. The conditions represented by Equations (18) and (19) are used to implement the switched alpha/beta tracker.

$$\text{If} \quad \sqrt{(\bar{\delta}^2_{x,k} + \bar{\delta}^2_{y,k} + \bar{\delta}^2_{z,k})} < TR, \text{ then } X_k^{display} = \bar{X}_k \ , \qquad \text{Eq. (18)}$$

$$\text{and if} \quad \sqrt{(\bar{\delta}^2_{x,k} + \bar{\delta}^2_{y,k} + \bar{\delta}^2_{z,k})} \geq TR, \text{ then } X_k^{display} = X_k \ .$$

Here TR is the switching threshold. If the sum of the outputs of the three low-pass filters (one for each tracker in each coordinate axes) is less than the threshold value, filtered position data is displayed to the user. If the sum of the outputs of the three low-pass filters are greater than or equal to the threshold value, the tracker determines that the vessel is accelerating and unfiltered position data is presented to the user.

The advantages of using the switched alpha/beta tracker are that the switched tracker allows the use of a small value for alpha during periods of no user acceleration, and retains the noise reduction capabilities of the conventional alpha/beta tracker. At the same time the user will have a reduced, but still acceptable, accuracy in the position output during periods of acceleration.

2.2 THE KALMAN FILTER

2.2.1 Kalman Filter Operation

An alternate method of converting pseudorange measurements into filtered position estimates is to pass them through a Kalman filter. A Kalman filter is a minimum error covariance estimator. That is, for situations where the noise to be filtered is Gaussian and has a zero mean, the error in the user's state will have the minimum possible covariance. In cases where the noise is non-Gaussian, the Kalman filter is the optimal linear filter. Reference 4 contains a detailed explanation of the Kalman filter. The Kalman filter is implemented using vectors and matrices rather

than scalars as used in the alpha/beta tracker. The first vector in a Kalman filter is the user-state vector

$$\bar{X}_k = \left[\bar{X}_k \quad \bar{\dot{X}}_k \quad \bar{Y}_k \quad \bar{\dot{Y}}_k \quad \bar{Z}_k \quad \bar{\dot{Z}}_k \quad \bar{T}_k \quad \bar{\dot{T}}_k\right]^T \qquad \text{Eq. (19)}$$

Here the superscript T denotes transpose. The state vector completely describes the user's filtered position, velocity, clock error and clock error rate. This is a vector expression of the quantities which were determined separately when using an alpha/beta tracker.

The next matrix of interest is the transition matrix

$$\Phi = \begin{bmatrix} 1 & \Delta T & 0 & 0 & 0 & 0 & 0 & 0 \\ & 1 & 0 & 0 & 0 & 0 & 0 & 0 \\ & & 1 & \Delta T & 0 & 0 & 0 & 0 \\ & & & 1 & 0 & 0 & 0 & 0 \\ & & & & 1 & \Delta T & 0 & 0 \\ & 0 & & & & 1 & 0 & 0 \\ & & & & & & 1 & \Delta T \end{bmatrix}$$

Here, ΔT is the time interval between pseudorange measurements. The transition matrix, when multiplied by the state vector, yields the predicted state vector for the next time period

$$\hat{\bar{X}}_{k+1} = \Phi \bar{X}_k \qquad \text{Eq. (20)}$$

where

$$\hat{\bar{X}}_{k+1} = \left[\hat{X}_{k+1} \quad \hat{\dot{X}}_{k+1} \quad \hat{Y}_{k+1} \quad \hat{\dot{Y}}_{k+1} \quad \hat{Z}_{k+1} \quad \hat{\dot{Z}}_{k+1} \quad \hat{T}_{k+1} \quad \hat{\dot{T}}_{k+1}\right]^T$$

If Equation (20) is evaluated, it may be seen that

$$\hat{X}_{k+1} = \bar{X}_k + \Delta T \, \bar{\dot{X}}_k, \qquad \text{Eq. (21)}$$

and

$$\hat{\dot{X}}_{k+1} = \hat{\dot{X}}_k. \qquad \text{Eq. (22)}$$

The Kalman filter and alpha/beta tracker use the same second order model for user motion. Therefore, Equations (21) and (22) are, with a single exception, the same

prediction equations used in the alpha/beta tracker. The single difference between the two sets of equations is that the alpha/beta tracker uses the receiver update period (T_{up}) as the interval between the k^{th} and $k+1^{th}$ states while the Kalman filter uses the time between pseudorange measurements (ΔT) as the interval between consecutive states. The reason is that the position calculation and alpha/beta tracker combination wait for a complete set of pseudorange measurements before computing and filtering the user's position. The Kalman filter, on the other hand, estimates a new user's position each time it receives a new pseudorange measurement.

Based upon the predicted state vector ($\overset{\Delta}{X}_k$) and the known position of the satellite to which a pseudorange is about to be measured, the filter computes the predicted range to the satellite ($\hat{P}_k$). When the Kalman filter receives the measured pseudorange (P_k) from the receiver module, it computes the difference between the predicted and measured pseudorange. This difference is known as the residual (P^R).

$$P^R = (P_k - \hat{P}_k) \qquad \text{Eq. (23)}$$

Based on the magnitude of the residual, the filter adjusts its predicted state matrix to create the new state matrix as shown in Equation (24).

$$X_k = \overset{\Delta}{X}_k + K\, P^R \qquad \text{Eq. (24)}$$

K is the Kalman gain vector and is of the form:

$$K = \left[K_x \; K_{\dot{x}} \; K_y \; K_{\dot{y}} \; K_z \; K_{\dot{z}} \; K_T \; K_{\dot{T}}\right]^T$$

There is a similarity between Equation (24) and Equations (6) and (7). The expression ($X_k - \overset{\Delta}{X}_k$) in the latter equations is equivalent to the residual in Equation (24). In Equation (7), ($\bar{\dot{X}}_{(k-1)}$) is equivalent to the predicted user velocity ($\hat{\dot{X}}_k$).

The Kalman gain vector transforms a pseudorange residual into a change in the predicted state vector. Two separate functions are performed in making this transformation. The first is a coordinate transformation function and the second is a weighting function.

The coordinate transformation function allows the Kalman filter to transform a pseudorange residual, which is a single dimension vector in the line of sight from the user to the satellite, into a change in the state vector, which is an 8-dimensional vector in the X, Y, Z, and T axis. Figure 2-5 illustrates this function.

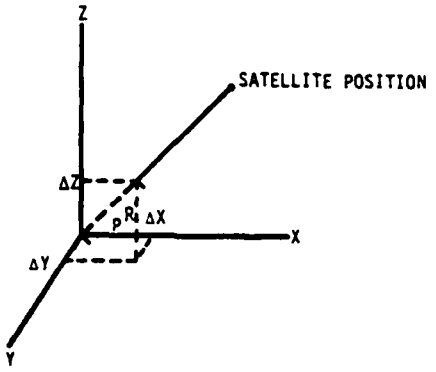

FIGURE 2-5. PSEUDORANGE TO USER STATE:COORDINATE TRANSFORMATION

For an incremental residual (P^R):

$$\Delta X = P^R \cos\theta_x \qquad \text{Eq. (25)}$$

$$\Delta Y = P^R \cos\theta_y \qquad \text{Eq. (26)}$$

and $$\Delta Z = P^R \cos\theta_z. \qquad \text{Eq. (27)}$$

The angles between the line-of-sight vector from the satellite to the user and the positive X, Y, and Z axes respectively are θ_x, θ_y, and θ_z .

The coordinate transformation for the clock error terms equals 1, because a change in the residual can be directly related to an equal change in the clock error.

The Kalman gain vector also serves a weighting function similar to the alpha and beta in the alpha/beta tracker, in which it determines the magnitude of change in the predicted state vector for a given residual. For example, if alpha has a value of 0.3 and the residual is +2, 0.6 may be added to $\hat{X}_k$ to calculate X_k. The terms of the Kalman gain vector function in the same way.

The terms of the Kalman gain vector, if rewritten as the product of a weighting term and a coordinate transformation term, are:

$$K = [w_x \cos\theta_x \quad \dot{w}_x \cos\theta_x \quad w_y \cos\theta_y \quad \dot{w}_y \cos\theta_y \quad w_z \cos\theta_z \quad \dot{w}_z \cos\theta_z \quad w_T \quad \dot{w}_T]^T$$

The w's are the weighting terms and the cosines are the coordinate transformation terms.

The weighting terms determine the magnitude of change in the predicted state vector for a given residual. This residual is the difference between the magnitude of the predicted pseudorange and the magnitude of the measured pseudorange. The difference is caused by process noise and measurement noise.

Figure 2-6 illustrates the relationship between process and measurement noise and how they affect the predicted, actual, and measured pseudoranges. Any difference between the predicted and actual pseudoranges is due to process noise. Because unmodeled variations in satellite motion and in the propagation velocity of signals through the atmosphere are ignored, the process noise equals the unmodeled vessel dynamics. Because a zero acceleration model is utilized for user motion and clock error when predicting the user's state, the primary contributor to process noise will be user and clock error acceleration. Any difference between the actual and measured pseudorange is due to the effect of measurement noise. The measurement noise equals the receiver's code chip error.

The desired output of the Kalman filter is the best possible estimate of the user's state. Therefore, since process noise causes the user's state to differ from the user's predicted state, the filter should pass as much process noise through the filter as possible. The passing of the process noise through the filter will enable the filter to more accurately estimate the user's state. However, since measurement noise can cause the filter to incorrectly estimate the user's state, the Kalman filter should filter out as much measurement noise as possible.

Unfortunately, the measurement noise and process noise both manifest themselves as noise in the measured pseudorange. If the weighting factor in the Kalman gain vector is small, causing the filter to discriminate against measurement noise, it will also discriminate against process noise. If the weighting factor is large, a great deal of

both process and measurement noise will pass through the filter. Therefore, if the measurement noise is large compared to the process noise, the accuracy gained in filtering out measurement noise will exceed the accuracy lost in filtering out process noise and the weighting factors should be small. However, if the process noise is much greater than the measurement noise, the accuracy gained in passing the process noise will exceed the accuracy lost in passing the measurement noise and the weighting factors should be large. The computation of the weighting factors in the Kalman gain vector represents a compromise between passing process noise through the filter and filtering out measurement noise.

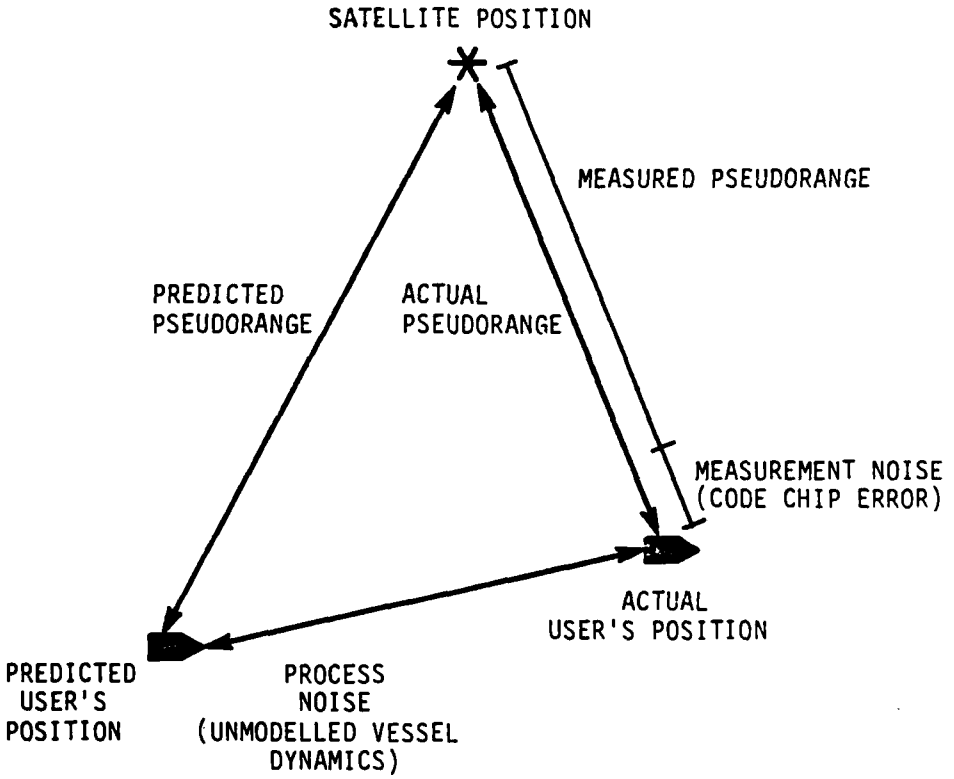

FIGURE 2-6. RELATIONSHIP BETWEEN PROCESS NOISE AND MEASUREMENT NOISE AND THEIR EFFECT ON PREDICTED, ACTUAL, AND MEASURED PSEUDORANGES

In order to compute the complete Kalman gain vector, we must define several new matrices. The first of these is the measurement noise matrix (R). Assuming the use of a sequential receiver, which limits us to incorporating one pseudorange measurement at a time, R reduces to a scalar. The term in R is the expected variance

of the measurement noise and is called the measurement noise covariance. For this study, we will use a measurement noise covariance equal to the expected code chip error variance (σ_ξ^2).

The next matrix to be defined is the process noise matrix (Q). The individual terms are called the process noise covariances and represent the expected covariance of the process noise in each dimension of the user's state. If it is assumed that there is no cross correlation between noise in each dimension of the user's state, then all of the diagonal terms of the matrix are zero and Q becomes:

$$Q = \begin{bmatrix} \sigma_x^2 & & & & & & & \\ & \sigma_{\dot{x}}^2 & & & & & & \\ & & \sigma_y^2 & & & & & \\ & & & \sigma_{\dot{y}}^2 & & & & \\ & & & & \sigma_z^2 & & & \\ & & & & & \sigma_{\dot{z}}^2 & & \\ & & & & & & \sigma_T^2 & \\ & & & & & & & \sigma_{\dot{T}}^2 \end{bmatrix}$$

Here σ_x^2 is the expected variance of the measurement-to-measurement noise in the position of the user in the X coordinate, with the other terms being similarily defined.

For this study, σ_x^2, σ_y^2, σ_z^2, and σ_T^2 will be set to zero. This is based upon the premise that the process noise in these terms can all be attributed to process noise in the velocity terms ($\dot{X}$, $\dot{Y}$, $\dot{Z}$, $\dot{T}$). The process noise covariance for the velocity terms will be set equal to the square of the product of the pseudorange sample period (Δ T) and the maximum expected acceleration in the axis of interest. This product equals the maximum expected unmodeled change in any velocity term during a single sample period. The relative magnitudes of the Q and R determine the weighting properties of the Kalman gain vector.

The final matrix to be defined is the observation matrix (H). As a result of our assuming that we are using a sequential receiver, H reduces to a vector. H is redefined for each pseudorange measurement using a new user or satellite position and is

$$H = [\cos\theta_x \quad 0 \quad \cos\theta_y \quad 0 \quad \cos\theta_z \quad 0 \quad 1 \quad 0].$$

The observation matrix determines the coordinate transformation properties of the Kalman gain vector.

The Kalman gain vector is recalculated using Equations (28) through (30) prior to incorporating each successive pseudorange measurement into the state vector.

$$P(-) = \Phi P(+) \Phi^T + Q \qquad \text{Eq. (28)}$$

$$\text{IK} = P(-) H^T (HP(-) H^T + R)^{-1} \qquad \text{Eq. (29)}$$

$$P(+) = (I - \text{IK}H) P(-) \qquad \text{Eq. (30)}$$

P(-) and P(+) are dummy matrices used in intermediate steps in the calculation. P(+) is initialized to Q when the Kalman filter is initialized.

The actual implementation of the Kalman filter is shown in the flowchart in Figure 2-7. The implementation shown incorporates a three satellite solution and was derived from the implementation contained in Chapter 2 of Reference 5. The assumed distance from the user to the center of the earth is incorporated into the solution by simulating the presence of a satellite at the center of the earth. The pseudorange to the earth centered satellite (P_{ecs}) is always equal to the radius of the earth. This pseudorange is incorporated into the solution immediately after the incorporation of each measure pseudorange. When incorporating (P_{ecs}), the time since the last pseudorange measurement (ΔT) is set equal to zero so the transition matrix Φ equals the identity matrix, and Q and R are set equal to zero.

2.2.2 Kalman Filter Performance

While there is no convenient set of equations (such as Equations (10) through (12)) with which to predict the performance of the Kalman filter, the performance can be analyzed using the same rationale used to analyze the alpha/beta tracker.

Since the Kalman filter and the alpha/beta tracker both use the same second order model of user motion when predicting the user's position, the Kalman filter output may be expected to contain a bias error whenever the user accelerates. As R is increased or Q decreased, the filter will increase the weighting on the predicted state vector and decrease the weighting on the residual calculated from the pseudorange

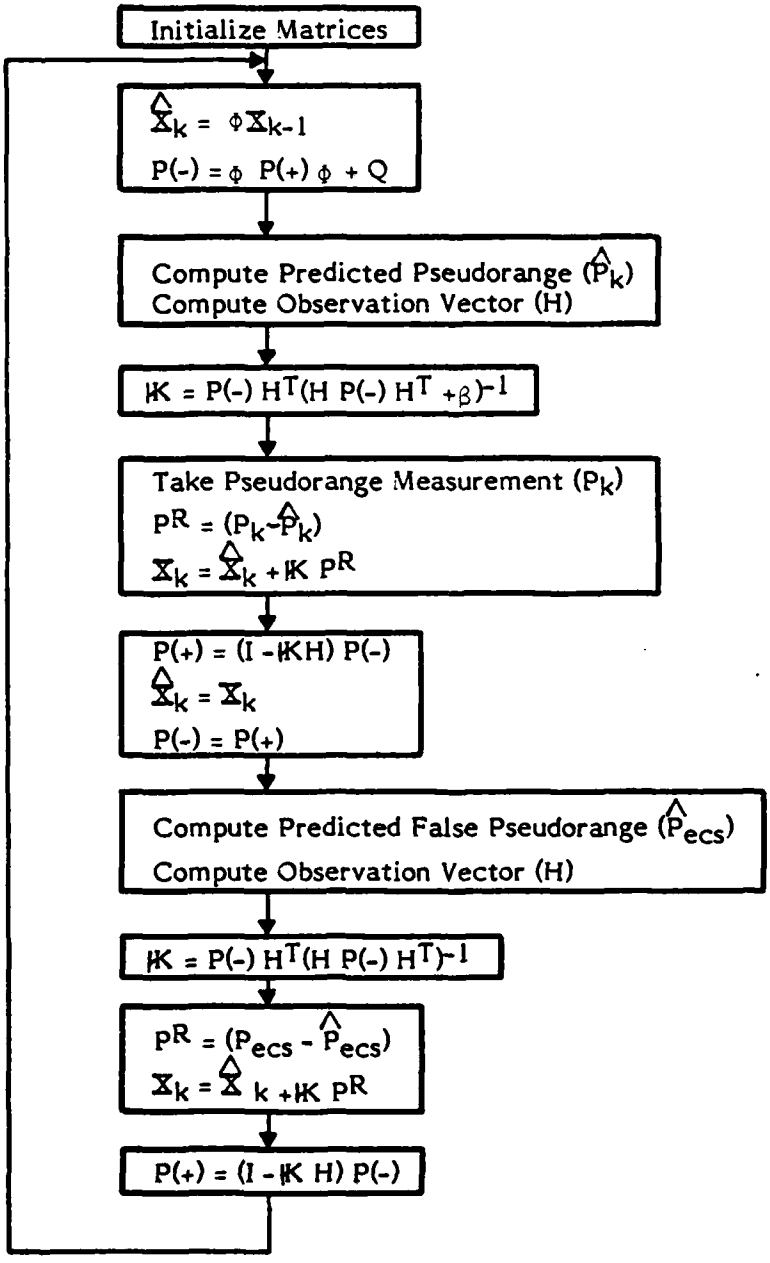

FIGURE 2-7. KALMAN FILTER IMPLEMENTATION FLOWCHART

measurement. Therefore, the noise in the output would be expected to be reduced and the bias error in the output to be increased. Conversely, when Q is increased or R decreased, the output noise would be expected to increase and the output bias error to decrease.

However, for any given level of noise reduction, the Kalman filter output may be expected to contain less acceleration-induced bias error than would be contained in the output of a standard alpha/beta tracker. The reason for this is that the Kalman filter incorporates individual pseudorange measurements as they are received, while the alpha beta tracker incorporates unfiltered position data only after a complete set of pseudorange measurements are received. Therefore, the Kalman filter can detect user acceleration in one third the time required by the alpha/beta tracker. This effectively cuts the filter's update time by a factor of three. Since the magnitude of the acceleration-induced bias error is proportional to the square of the filter update time, the bias error would be expected to be reduced by a factor of 9. This should allow the Kalman filter to retain a high level of noise reduction without creating significant acceleration induced bias error.

2.3 POSITION ERRORS DUE TO SWITCHING TRANSIENTS AND ALTITUDE INPUT ERRORS

There are two types of position errors which are of special interest. The first type is the result of an incorrect assumption of the user's altitude when using a three satellite solution. The second type is the transient error which occurs when the receiver switches satellite constellations and the pseudoranges of some of the satellites involved in the switch have large bias errors.

2.3.1 Errors Caused By An Incorrect User Altitude Assumption

There are four unknowns for which most navigation processors must solve. They are the user's position in three dimensions and the user's clock error. In order to solve for these four unknowns using the pseudoranges to only three satellites, the navigation

processor must make use of some other information. Most often, the other bit of information used is the user's assumed altitude. In this case, the user's altitude is defined as the sum of the radius of the earth at the user's position and the height of the user's antenna above the surface of the earth. If the estimate of the user's altitude is in error, an error will exist in the user's calculated position. The magnitude of this error will depend upon the geometry of the satellite constellation being tracked and the magnitude of the error in the altitude estimate.

The three-satellite solution will position the user somewhere on a hyperbola. When an assumed altitude is incorporated, the user's position is narrowed down to the intersection of the hyperbola and a sphere centered at the center of the earth and with a radius equal to the user's assumed altitude (Figure 2-8).

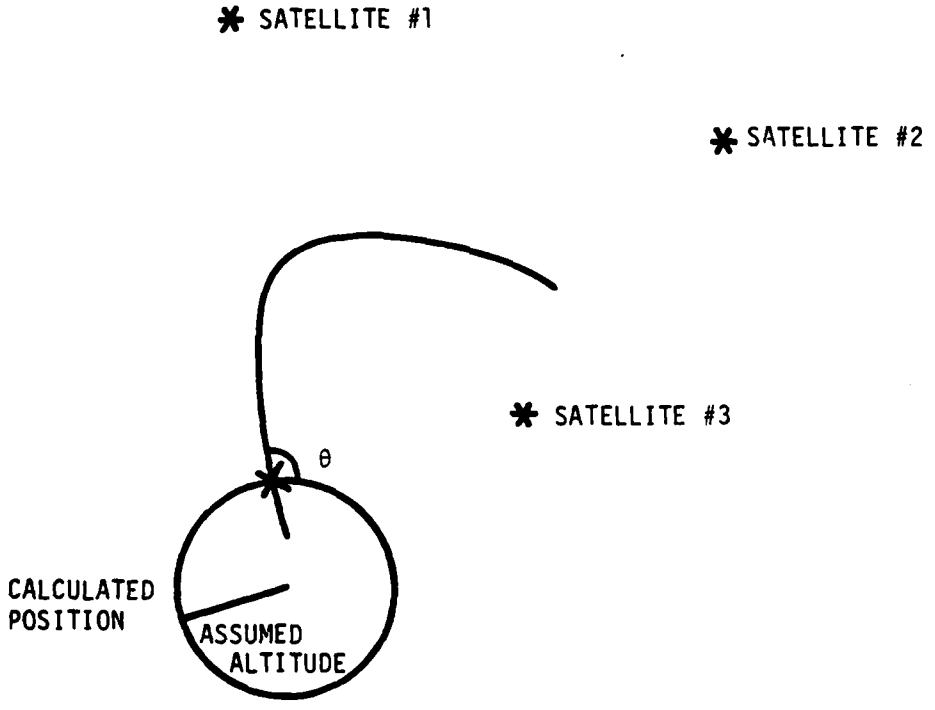

FIGURE 2-8. GEOMETRY OF POSITION SOLUTION USING THREE SATELLITES AND ASSUMED ALTITUDE

If the user's assumed altitude is changed, the position of the user in the horizontal plane at his location will change. For small deviations in assumed altitude, where the

surface of the sphere can be approximated by a plane and the arm of the hyperbola can be approximated by a line, the position change in the horizontal plane can be calculated from

$$\Delta H = \Delta A \cot\theta \qquad \text{Eq. (31)}$$

Here ΔH is the change in the horizontal position, ΔA is the change in assumed altitude, and Θ is the angle between the line approximating the arm of the hyperbola and the plane approximating the surface of the sphere. Therefore, if the user's assumed altitude is in error by ΔA, the user's calculated position can be expected to have a bias error of ΔH. An analysis of the expected range of θ at any position, the accuracy required by the user, and the accuracy with which the user can estimate his altitude will determine whether or not the use of a three satellite solution is acceptable.

2.3.2 Transient Position Errors Due to Satellite Constellation Switching

If the pseudorange to a satellite being tracked by a receiver has a bias error associated with it and the pseudorange is passed uncorrected to the navigation processor module, then the user's calculated position will contain a bias error. If each satellite has a bias error associated with its pseudorange, then each satellite constellation will have a particular user's calculated position bias error associated with it. A satellite constellation is considered here to be composed of a set of three satellites which could be tracked by the receiver. If the receiver switches from tracking one constellation to tracking another constellation, a transient will appear in the user's calculated position at the output of the navigation processor module as the navigation processor switches from calculating a position containing one bias error to calculating a position containing another bias error. That is, the bias errors associated with the pseudoranges to a particular constellation of satellites form a vector input to the navigation processor module. This vector input creates a position bias error, which is a vector at the output of the navigation processor module. The switching from one satellite constellation to another creates a step change in the pseudorange bias error vector input to the navigation processor module. The transient in the position bias error output vector will therefore be the step response of the navigation processor module.

The step response of the navigation processor module is determined by the step response of the alpha/beta tracker or Kalman filter which is being used. It is assumed that the position calculation algorithm will pass a step function without affecting it. Both the alpha/beta tracker and the Kalman filter used in this study have slightly underdamped step responses. This allows them to respond quickly to a step function at their inputs with only minimal overshoot (typically less than 10 percent). As long as the trackers or filters used to filter position data do not have step responses which are oscillatory or have large overshoots, the overshoot in the position error transients at the output of the navigation processor module will not significantly degrade the accuracy of the position data.

3. NAVIGATION PROCESSOR SIMULATION PROGRAM RESULTS

A navigation processor simulation program was developed in order to compare the operation of the alpha/beta trackers and the Kalman filter described in the preceding section. A description of the simulation program is contained in Appendix C. In this section, the initial conditions used in running the program and the measured outputs of the program will be described. The actual results obtained will then be presented and compared with the expected results.

The simulation program starts with the simulated vessel at the position Lat. 45° North, Lon. 45° West, with a system time of 1300 seconds. The ship steams on a course of 000° T at a speed of 10 knots for 100 receiver update periods. It then commences a 90° turn to starboard. The radius of the turn is 300 meters. The turn-induced acceleration is 0.006 G's. Upon completing the turn, the ship steams on a course of 090° T for 50 receiver update periods. The receiver update period is fixed at 5.4 seconds for all runs. The simulated ship roll angle is 5° and the height of the antenna above the ship's center of rotation is zero. All the runs start with an initial user clock error of one microsecond and a clock stability of one part in ten million.

During the first 25 receiver update periods in a run, no alpha/beta tracker or Kalman filter is used to filter data. This period allows the navigation processor to settle on the user's position and clock error without having the excessive oscillation which would result if a cold start computation were fed into the tracker or filter. After the initial cold start period, the tracker or filter is incorporated into the processor. Twenty-five additional update periods are allowed for the tracker or filter to settle on the user's position and clock error. At the end of this tracker settling period, 50 update periods remain until the ship enters its turn.

These 50 update periods immediately preceeding the commencement of the turn comprise the approach leg. The criterion function ($J_{\bar{x}}$) is computed for this leg and is used as the measure of accuracy during a zero acceleration condition. Upon completing the approach leg the ship enters its turn and takes approximately 17 update periods to complete the turn. The mean horizontal position data error during this time is used as the measure of the acceleration induced bias error. These quantities are calculated for each run of the simulation program.

3.1 BASELINE AND ALPHA/BETA TRACKER RESULTS

This section covers four types of simulation runs. The first is a baseline run in which no alpha/beta tracker or Kalman filter is used to filter position data. In the other three runs, an alpha/beta tracker is used to smooth position data. The first run uses a tracker with an alpha of 0.3. The second run uses a tracker with an alpha of 0.8. The final run uses a switched tracker with an alpha of 0.3, a low pass filter constant of 0.5, and a switching threshold of 12 meters. The criterion function and bias during the second turn for each of these runs are shown in Table 3-1. Figures 3-1 through 3-4 contain graphs of the crosstrack and along-track position errors vs. time for each of these runs. The error plots up to 270 seconds show primarily error which results from the cold start procedure used in the simulation and should be ignored. The approach leg begins at 270 seconds, the turn begins at 540 seconds and ends at 631.6 seconds.

TABLE 3-1. APPROACH LEG CRITERION FUNCTION AND BIAS ERROR DURING TURN

Type of Tracker	α	Γ	TR	$J_{\bar{x}}$	Bias
none	-	-	-	12.8	.67
normal	.3	-	-	6.1	10.5
normal	.8	-	-	10.8	1.8
switched	.3	.5	12	6.7	2.3

Table 3-1 shows that a significant noise reduction can be accomplished using a low alpha tracker. (α =.3) However, as expected, a penalty in the form of a bias error is incurred during the turn. The tracker with an alpha of 0.8 shows very little noise reduction and very little acceleration-induced bias error. The switched alpha/beta tracker shows significant noise reduction with very little bias error during the turn.

If Figure 3-1 is compared with Figure 3-2, noise reduction accomplished during the approach leg when using an alpha of 0.3 is apparent. Equally apparent is the large bias error induced during the turn. While the mean bias error was calculated as 10.5 meters, the peak bias exceeds 30 meters. Figure 3-3, which is the plot generated using a normal tracker with an alpha of 0.8, shows very little noise reduction during the approach leg and very little bias error during the turn. Figure 3-4, which was generated using a switched tracker shows significant noise reduction during the approach leg. As the

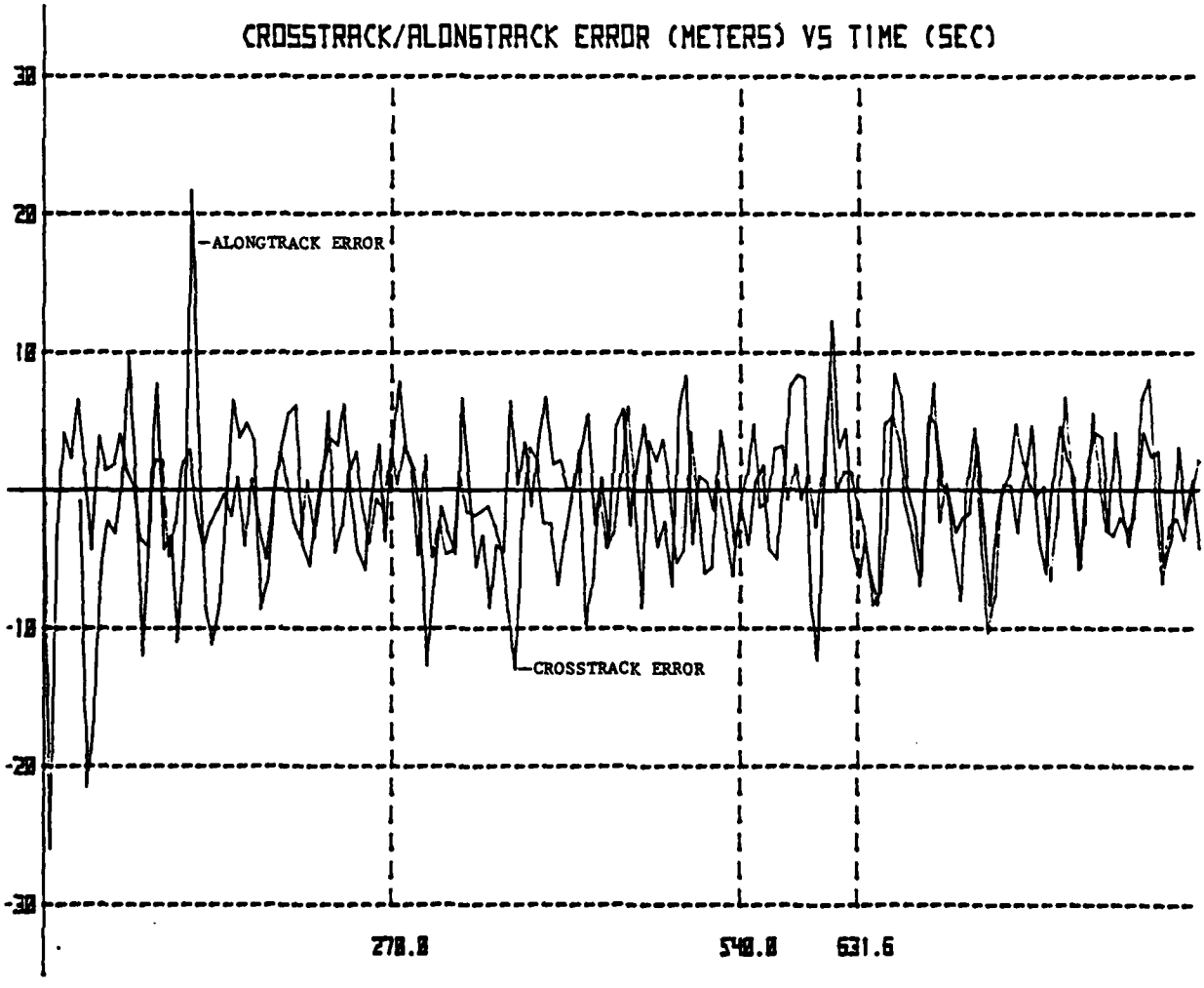

FIGURE 3-1. SIMULATION PROGRAM RESULTS WITH NO TRACKER

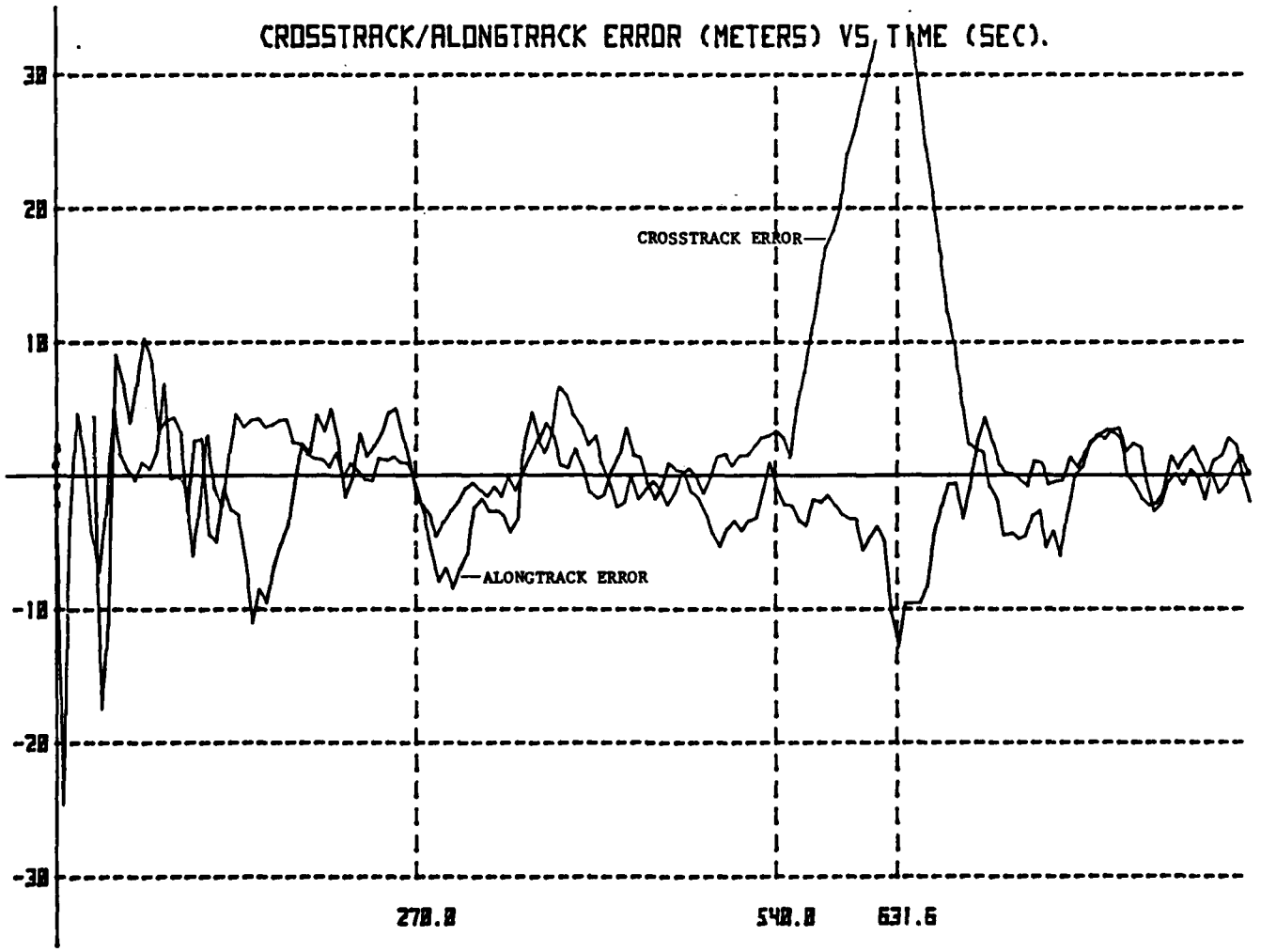

FIGURE 3-2. SIMULATION PROGRAM RESULTS WITH NORMAL TRACKER ($\alpha = 0.3$)

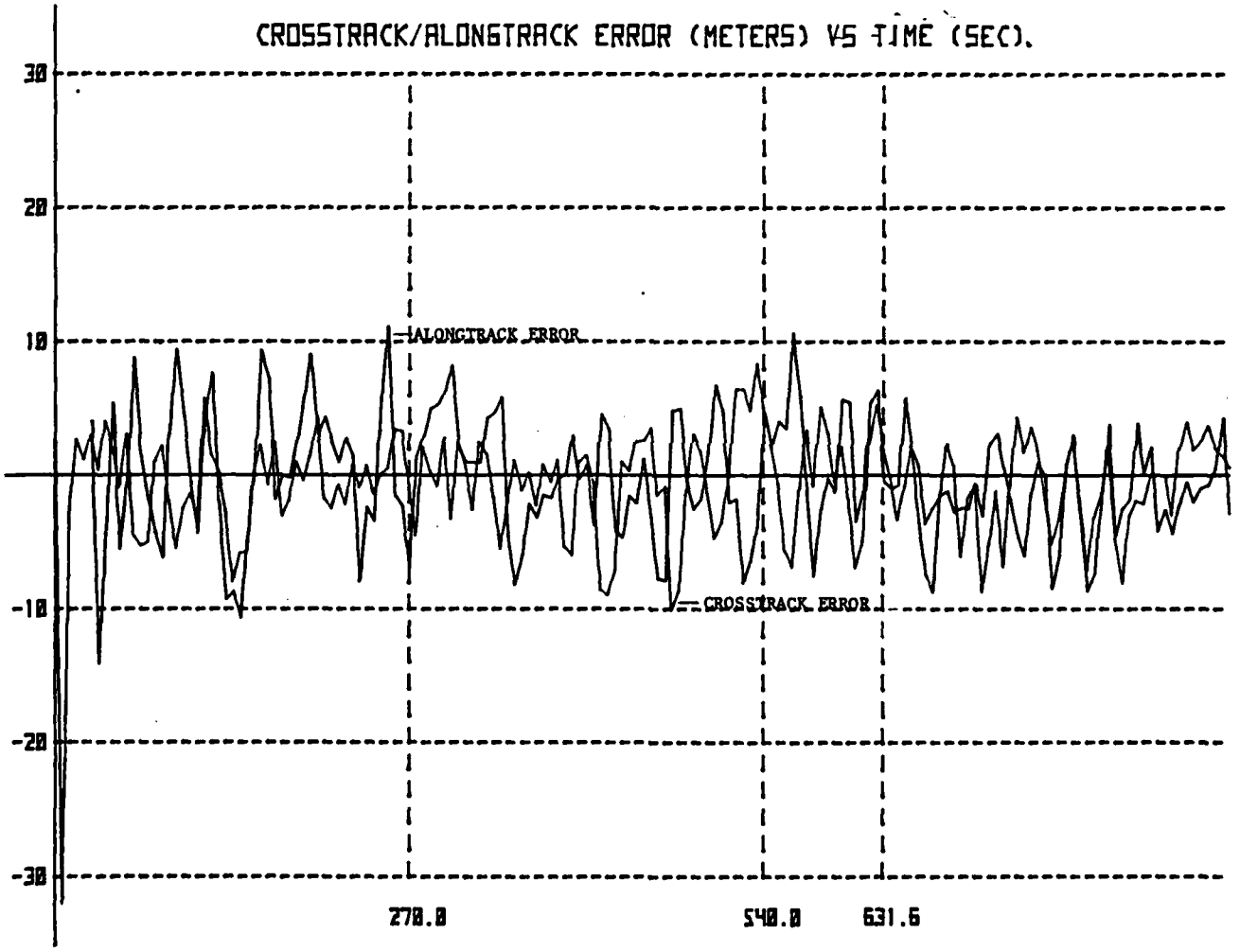

FIGURE 3-3. SIMULATION PROGRAM RESULTS WITH NORMAL TRACKER (α = 0.8)

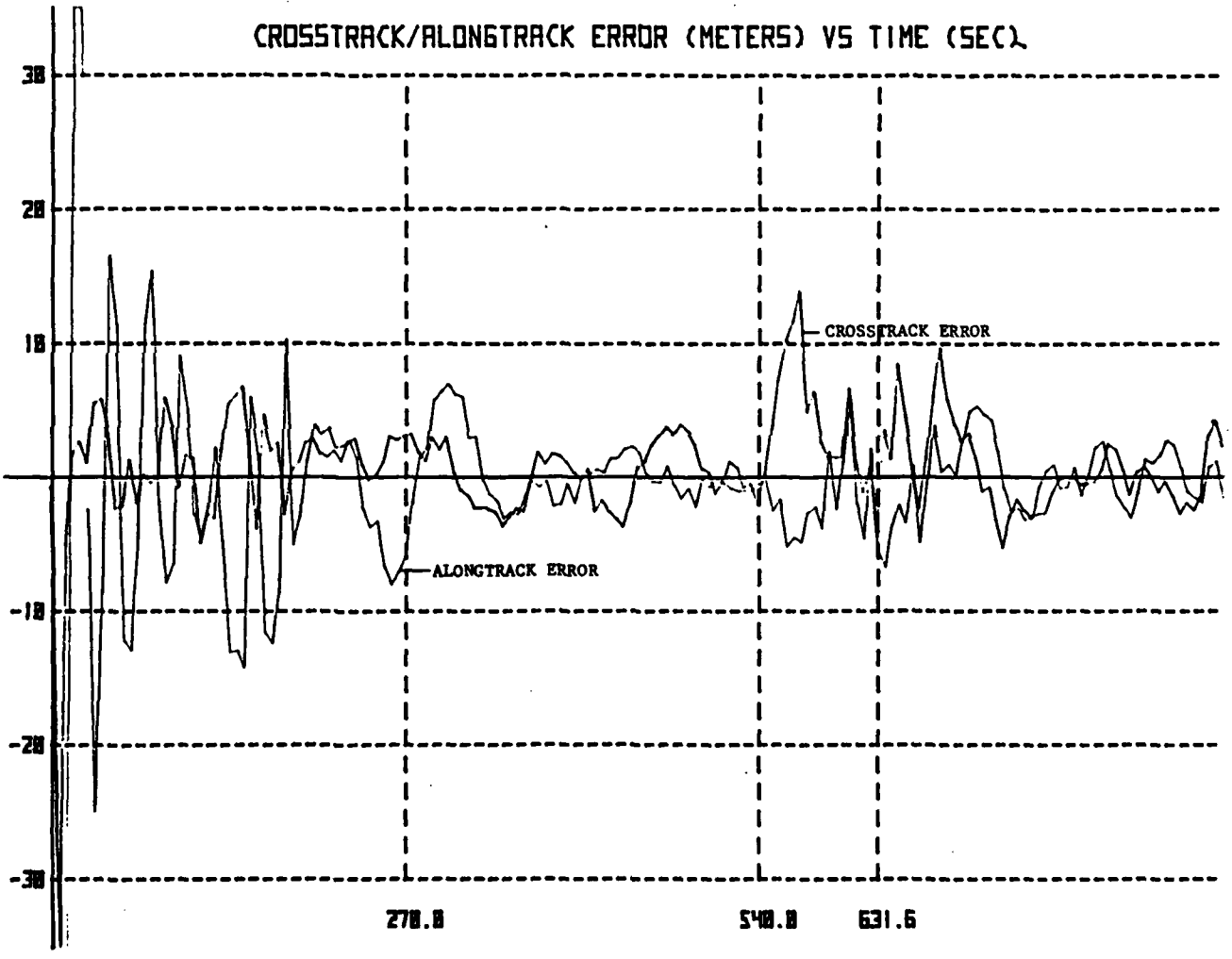

FIGURE 3-4. SIMULATION PROGRAM RESULTS WITH SWITCHED TRACKER

bias begins to grow after the ship enters its turn, the tracker switches to displaying unfiltered data. This data has little bias error but the magnitude of the noise present is greater than that present in the filtered data. After the ship completes its turn and the bias error in the filtered data falls below the switching threshold, the filter switches back to displaying filtered data. The performance of all these filters is consistent with the performance that was expected.

3.2 KALMAN FILTER RESULTS

This section contains results generated when running the simulation program using a Kalman filter. There are three filter parameters which were varied. They are measurement noise covariance, user velocity noise covariance, and user clock frequency noise covariance. The values which were used for these parameters were chosen to span the range of expected values for the measurement noise, user velocity noise, and user clock frequency noise.

The measurement noise covariance is the term in the R matrix. The value of this term is the same for each of the 3 active satellites. The value of this term for the earth centered satellite was zero. As the measurement noise covariance term is increased, the filter is expected to place more weight on the predicted state vector and less weight on the residual. This will increase the amount of filtering, which should decrease J_x but should increase the bias error during the turn. Table 3-2 shows the results of runs made with a Velocity Noise Covariance of 0.1 $(\text{meters/sec})^2$, a Frequency Noise Covariance of 3.9 $(\text{meters/sec})^2$, and various values for the Measurement Noise Covariance.

TABLE 3-2. CRITERION FUNCTION AND BIAS DURING TURN VS. MEASUREMENT NOISE COVARIANCE $(\text{METERS/SEC})^2$

Measurment Noise Covariance	$J_{\bar{x}}$	Bias
7.93	7.96	1.08
15.00	7.33	1.73
50.00	6.38	2.00
81.00	5.93	3.00
121.00	5.73	3.23

Table 3-2 shows the expected decrease in J_x and increase in the bias error during the turn as the measurement noise covariance is increased.

The user velocity covariance terms are the second, fourth, and sixth diagonal term of the process noise matrix (Q). These terms represent the expected covariance of the noise in the user's velocity in each of the three position axes. As the velocity noise covariance increases, the filter places more weight on the residual and less weight on the predicted state vector. This will decrease the amount of filtering, which should increase J_x and decrease the bias error during the turn. An additional change which will take place as the velocity noise covariance increases is that the percentage of the residual which is accounted for by changes in the position and velocity terms of the state vector increases relative to the amount which is accounted for by changes in the clock error and frequency error terms of the state vector. The reason for this is that as the velocity noise covariance increases relative to the frequency noise covariance, the filter expects a greater percentage of the difference between the predicted and measured pseudarange to be a result of velocity noise as opposed to clock frequency noise. However, the effect of this change is minor when compared to the earlier weighting change. Table 3-3 shows the results of runs made with a Measurement Noise Covariance of 7.93 meters^2, a Frequency Noise Covariance of 3.9 (meters/sec)^2, and various values for the Velocity Noise Covariance.

TABLE 3-3. CRITERION FUNCTION AND BIAS DURING TURN VS. VELOCITY NOISE COVARIANCE (METERS/SEC)^2

Velocity Noise Covariance	$J_{\bar{x}}$	Bias
.01	5.93	2.53
.05	6.63	1.43
.10	7.93	1.08
.50	8.63	.30
1.00	10.00	.77

As expected, the criterion function increases as the velocity noise covariance is increased. However, contrary to expectations, the bias errors do not continually decrease as the velocity noise covariance increases. The bias error for a velocity noise covariance of 0.50 is smaller than the bias error for a velocity noise covariance of 1.00. A satisfactory explanation for this deviation has not been found.

The final term to be manipulated is the clock frequency noise covariance. This is the eighth diagonal term in the process noise matrix. The primary effect of increasing this term is to increase the percentage of the residual. This is accounted for by changing the clock error and clock frequency error terms of the state vector relative to the percentage, which is accounted for by changing the position and velocity terms of the predicted state vector. This effect will be relatively minor. The weighting of the residual vs. the predicted state vector will not change significantly as there will be no large changes in the criterion function or the bias error. Table 3-4 shows the results of runs made with a Measurement Noise Covariance of 7.93 meters^2, a Velocity Noise Covariance of 0.1 (meters/sec)^2 and various values for the Frequency Noise Covariance.

TABLE 3-4. CRITERION FUNCTION AND BIAS DURING TURN VS. FREQUENCY NOISE COVARIANCE (METERS/SEC)^2

Frequency Noise Covariance	$J_{\bar{x}}$	Bias
.1	7.69	.60
1.0	7.82	1.00
3.9	7.64	.85
8.0	7.69	.94
16.0	7.93	1.08

These results are as expected. As a final check, all three terms were changed at once holding the ratios between the three constant. There will be no significant changes in the criterion function or bias error as the values change. The reason for this is that if the measurement and process noise are increased by the same factor, the relative weighting of the residual and the predicted state vector will not change. Table 3-5 shows the results of the runs made when changing all three terms. With the exception of the criterion function for the second set of runs, these results are as expected. As with the unexpected deviation present in the data in Table 3-3, a satisfactory explanation of the deviation in Table 3-5 has not been found.

The results obtained using a Kalman filter show that the Kalman filter is capable of matching or exceeding the performance of an alpha/beta tracker with respect to both accuracy during no-acceleration conditions and lack of bias error during conditions involving accelerations. The proper selection of the covariance terms is critical to determining the level of filtering and therefore the amount of noise reduction achieved and the amount of bias error induced.

TABLE 3-5. CRITERION FUNCTION AND BIAS DURING TURN VS. ALL COVARIANCE TERMS

MEASUREMENT	COVARIANCES VELOCITY	FREQUENCY	$J_{\bar{x}}$	Bias
12.5	.0125	2.0	5.85	2.56
25.0	.0250	4.0	6.80	2.58
37.5	.0375	6.0	5.83	2.83
50.0	.0500	8.0	5.64	3.21
100.0	.1000	16.0	5.82	2.61
150.0	.1500	24.0	5.68	2.91
200.0	.2000	32.0	5.71	2.78

Figure 3-5 is a plot of the crosstrack error and along-track error vs. time generated using a Kalman filter with a Measurement Noise Covariance of 50 meters^2, a Velocity Noise Covariance of 0.1 (meters/sec)^2, and a Frequency Noise Covariance of 3.9 (meters/sec)^2. This example shows typical noise reduction capability of the Kalman filter and the simultaneous lack of significant bias error during the turn.

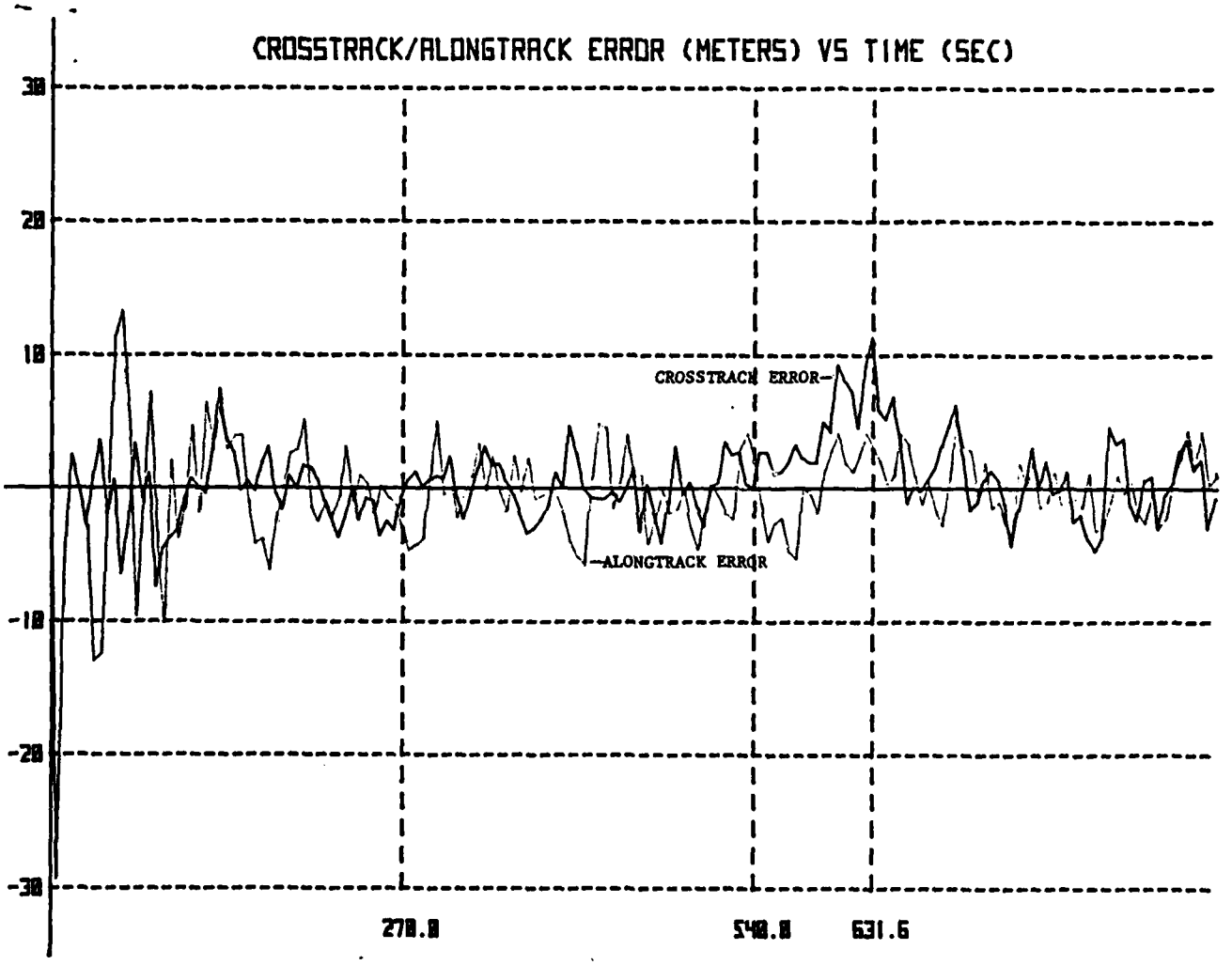

FIGURE 3-5. SIMULATION PROGRAM RESULTS WITH KALMAN FILTER

3.3 OTHER RESULTS

A set of runs were made with a 10-meter error in the assumed altitude of the user. The user was stationary and the simulation was run for a 24 hour period. As with all prior simulations, the user receiver evaluated the satellite constellation every two minutes and chose the optimum constellation to track. The simulation was run with the user at Lat. 45° North, Lon. 45° West and at Lat. 0° North, Lon. 0° West. The maximum horizontal bias error created by the 10-meter error in assumed altitude was 7.9 meters and the minimum bias error was 0.2 meters. Therefore, for the geometries simulated, the position bias error can be as large as 79 percent of the assumed altitude error. The user interested in highly accurate horizontal data must then be able to accurately estimate the distance from the center of the earth to his antenna. If the receiver has access to a written table for tidal variation and an accurate model of the earth, such as the WGS-72 geoid, then the user would have to enter only the antenna's height above the ship's waterline to make a highly accurate three-satellite solution possible. If such information is unavailable to the receiver, the three-satellite solution is not appropriate for use when highly accurate horizontal position information is needed.

Another set of runs were made in which the receiver switching between two satellite constellations, each with a large position bias error associated with it, was simulated. Rather then actually switching between constellations, a single constellation was used, and the bias error associated with the constellation was switched between two different values. This was accomplished by instantaneously changing the pseudorange bias error associated with one satellite. This allowed the effect due to large changes in the bias errors to be isolated from the effects due to different geometries such as changing HDOPs and changing Signal-to-Noise Ratios. The run was made using both a Kalman filter and an alpha/beta tracker. As expected, the transient at the output of the navigation processor was the step response of the filter. Figure 3-6 is a plot of the crosstrack and along-track bias errors vs. time for one of the runs using an alpha/beta tracker to filter the position data.

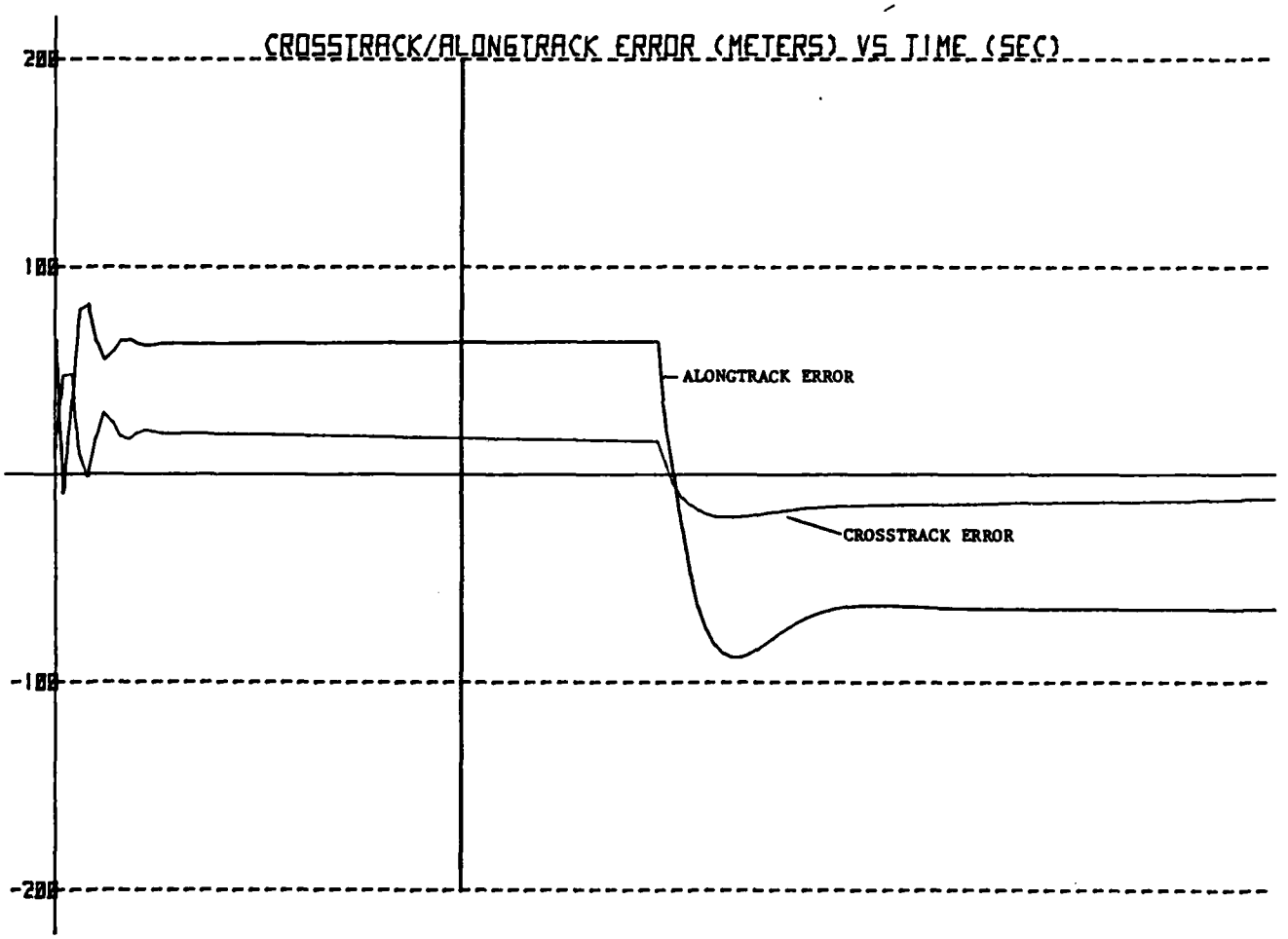

FIGURE 3-6. SIMULATION PROGRAM RESULTS USING ALPHA/BETA TRACKER WITH A SWITCH OF SATELLITE CONSTELLATIONS

4. CONCLUSIONS

The results presented in Section 3 lead to several conclusions. First, when Table 3-1 and Figures 3-1 through 3-4 are examined, it can be seen that the switched alpha/beta tracker performs better than either normal alpha/beta tracker in filtering position data during the approach leg without adding a significant bias error during the turn.

The results obtained when using a Kalman filter (Tables 3-2 through 3-5, Figure 3-5) show the expected increases and decreases in noise filtering and bias error as the measurement noise covariance and the process noise covariance (which is broken down into velocity and frequency noise covariances) are adjusted. The amount of noise filtering can be increased by increasing the measurement noise covariance or decreasing the velocity noise covariance. This also leads to an increased bias error. Adjusting the frequency noise covariance (Table 3-4) has little effect on the amount of filtering or the induced bias error. When all three covariances are changed so that their relative sizes remain constant (Table 3-5), neither the level of filtering nor induced bias error change significantly.

If the Kalman filter results are compared with the switched alpha/beta tracker results, it may be seen that the Kalman filter can simultaneously offer slightly more noise filtering with slightly less induced bias-error noise than the switched alpha/beta tracker.

The results generated when using an erroneous user altitude assumption show that the horizontal bias error (ΔH) can be a large percentage of the error in assumed altitude (ΔA). For the specific geometries which were simulated, this percentage ranged from 2 percent to 79 percent.

The final set of results was generated using a normal alpha/beta tracker with the receiver switching between satellite constellations having different position bias errors associated with them. The position error graph (Figure 3-6) shows the slightly underdamped response characteristic of the tracker. The overshoot does not significantly decrease the overall accuracy of the position data. However, if the user were using the tracker to provide velocity as well as position data, the transient could be a greater problem.

APPENDIX A. RECEIVER MODULE

This appendix addresses the performance tradeoffs which must be made when selecting GPS receiver module parameters, and is the result of work done by James Kuhn and the author. The only portion of the receiver module considered is the code tracking section. The code tracking section is preceded by an RF front end which scales, bandlimits, and amplifies the incoming signals. The signals received by the receiver module consist of a continuous carrier transmitted by each satellite at 1575.42 MHz. The carrier is modulated by the modulo-2 sum of a 1.023 MHz pseudorandom binary code known as a Gold Code and a 50 bps digital data stream. Binary phase shift keying modulation is used. The Gold Code is 1023 bits in length and is unique for each satellite.

The function of the receiver module is to read the 50 bps data stream present in each received signal, and to measure the arrival time of the beginning of each code sequence from each satellite. Using the data which tells when a given code sequence was transmitted by the satellite and the measured arrival time of that signal at the receiver, the receiver module computes the pseudorange to the satellite. This pseudorange is passed to the navigation processor module.

Because the Gold Code for each satellite is unique, a single receiver channel can track the signal from only one satellite at a time. Since this report will be concerned with only single channel receivers, all the receivers are assumed to be sequential rather than parallel in nature. That is, they will measure the pseudorange to a given satellite, then measure the pseudorange to the next satellite, etc. The performance of dual channel receivers will not be considered, because with an efficient channel time management scheme the performance of a single channel receiver can closely approximate that of a dual-channel receiver.

The channel time management scheme used in a receiver will determine the length of time that a channel can track any given satellite during an update period. As will be demonstrated later, this length of time, called the dwell time, will determine to a great extent the accuracy achievable by the receiver. Therefore, the choice of an efficient time management scheme is necessary to optimize receiver performance.

Figure A-1 shows the channel time management scheme used for this study. This scheme is modeled after the scheme developed by Stanford Telecommunications Inc.,

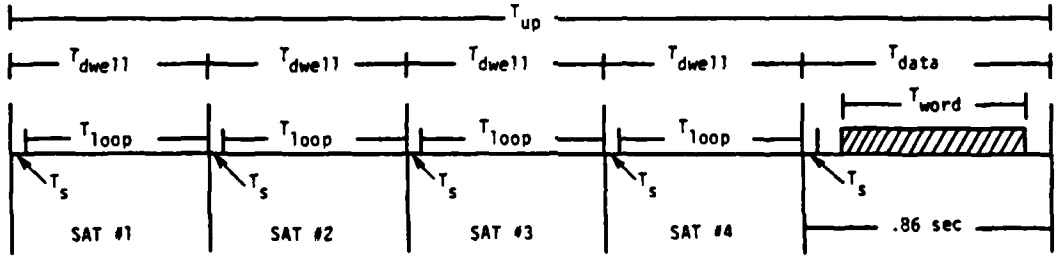

T_{up} = RECEIVER UPDATE INTERVAL

T_{dwell} = RECEIVER DWELL TIME ON EACH SATELLITE

T_{loop} = CODE TRACKING LOOP TRACKING AND SETTLING TIME

T_s = CODE TRACKING LOOP STARTUP TIME (40 mSec)

T_{data} = TIME ALLOCATED FOR RECEIVER TO GATHER DATA FROM ONE SATELLITE (.86 sec)

T_{word} = TIME REQUIRED FOR RECEIVER TO GATHER ONE DATA WORD OF 32 BITS (.64 sec)

THIS SCHEME SUPPORTS A 3 SATELLITE NAVIGATION SOLUTION. THE FOURTH SATELLITE IS TRACKED IN ORDER TO PROVIDE A SMOOTH TRANSITION WHEN ONE OF THE THREE ACTIVE SATELLITES PASSES OUT OF VIEW.

FIGURE A-1. TIME MANAGEMENT SCHEME FOR A SINGLE-CHANNEL RECEIVER

for MIT Lincoln Laboratory's Experimental Dual-Channel Receiver. This receiver was designed for aviation applications. The scheme shown in Figure A-2, an example of a more efficient time management scheme, makes possible accuracies which are 15 percent better than those achieved using the scheme shown in Figure A-1, and only seven percent worse than those achieved by a dual channel receiver. This scheme makes use of the longer dwell time which can, due to the relativly benign maneuvering characteristics of marine vessels, be associated with marine receivers. The scheme allows the receiver to read each satellite's 50 bps data stream during the dwell time for that satellite. Both time management schemes assume that the receiver is tracking three active satellites and one spare satellite.

During the dwell time for each satellite, the code tracking loop attempts to track the Gold Code being transmitted by the satellite. The code tracking loop within each receiver channel is assumed to be a Tau Dither Tracking Loop. Reference 6 contains a detailed description of the operation of the Tau Dither Loop and presents an expression for the accuracy achievable with the loop. This expression, modified to yield an answer in units of meters, is

$$\sigma_c = (293.9 \text{ meters}) \sqrt{\frac{B_L}{C/N_0} \left(905 + \frac{.453 - (10\ T_d\ B_{IF})^{-1}}{(1 - \Delta T/T_c)^2 \left(\frac{C/N_0}{B_{IF}} \right)} \right)} \quad \text{Eq.(A-1)}$$

σ_c is called the code chip error and is the steady-state, noise-limited code chip misalignment error for the code tracking loop., and is expressed in meters. It does not take into account residual error due to initial code loop offset.

B_{IF} is the loop filter bandwidth in Hz. As B_{IF} is decreased, σ_c decreases. However, the sensitivity of σ_c to changes in B_{IF} is small. Additionally, B_{IF} must be wide enough to pass without distortion the diffused carrier signal which still contains a 50 bps data stream. Using the rule of thumb given by Hartman (Ref. A-1) that B_{IF} shall be two to six times the data rate, B_{IF} was set at 200 Hz and this value will be used for the remainder of the study.

$\Delta T/T_c$ is the normalized dither step size. This represents the size in code chips (one code chip equals 977.5 nsec) of the offset the early and late codes which are fed into the correlator of the tracking loop. As $\Delta T/T_c$ decreases so does σ_c and the sensitivity of σ_c to changes in $\Delta T/T_c$ is small. The penalty paid for decreasing $\Delta T/T_c$ is a reduction in the capture and tracking range of the loop. $\Delta T/T_c$ was set at 0.5.

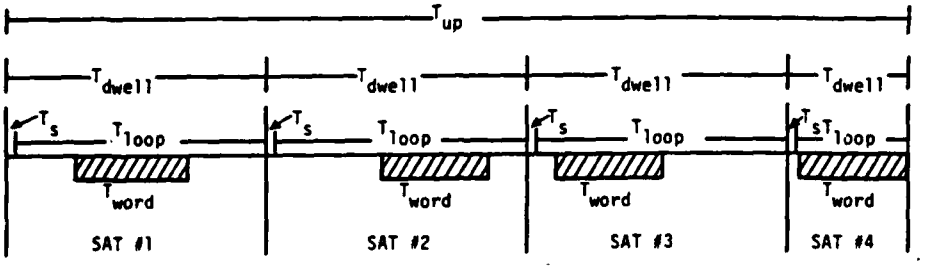

T_s = 40 m sec

$T_{dwell_{1,2,3}}$ = 1.56 sec

T_{dwell_4} = .72 sec

T_{word} = .64 sec

T_{up} = 5.4 sec

$T_{loop_{1,2,3}}$ = 1.52 sec

T_{loop_4} = .68 sec

FIGURE A-2. EXAMPLE OF AN ALTERNATIVE TIME MANAGEMENT SCHEME FOR A SINGLE-CHANNEL RECEIVER

T_d is the dither interval in seconds. This equals one half the reciprocal of the dither frequency. The dither frequency is the rate at which the Tau Dither loop correlator switches between the early and late version of the Gold Code. As T_d decreases so does σ_c. The sensitivity of σ_c to changes in T_d is very small and T_d was set at 0.01 seconds for this study.

C/N_o is the Carrier-to-Noise Power Density ratio. While normally expressed as dB-Hz, it must be converted to Hz before being used in the formula. (i.e., 40 dB-Hz equals 10^4 Hz) As C/N_o increases, σ_c decreases. σ_c is highly sensitive to changes in C/N_o. However, the designer has no direct control over C/N_o. The value for C/N_o used in this study is set to 38.5 dB-Hz for most satellites. When simulating a satellite whose elevation angle was less than the ship's roll angle plus 10 degrees, C/N_o was calculated as in the relation

$$C/N_o = 38.5 + .5\,(\text{elevation}\Delta - \text{roll}\Delta - 10^o). \qquad \text{Eq. (A-2)}$$

This expression simulates the expected reduction in C/N_o as the satellite signal falls lower and lower on the antenna pattern, which it is assumed will roll off at 0.5 dB/degree below 10^o elevation. The base figure of 38.5 dB-Hz is based on expected signal strengths of the transmitted signals.

The final parameter in Equation (A-1) is B_L. This is the tracking loop bandwidth expressed in Hz. As B_L decreases, so does σ_c, and σ_c is highly sensitive to changes in B_L. The designer is not free to choose an arbitrarily small B_L as would seem desirable in order to minimize σ_c.

At the beginning of each dwell period on any satellite, there is a high probability that the loop's estimate of the position of the satellite's Gold Code in time will contain an error. This error is known as a prepositioning error. During the dwell period the loop must be able to reduce the error in its estimate of Gold Code position and leave a residual code position error which is minimal. If the goal of having a residual error of less than 5 percent of the magnitude of the prepositioning error is arbitrarily set, and the code tracking loop is modeled as a first-order loop, then the minimum required bandwidth can be related to the loop tracking time (T_{loop}) as shown in the expression

$$B_L = \ln(.05)/(-4\,T_{loop}). \qquad \text{Eq. (A-3)}$$

This expression for the minimum allowed B_L is based on the transient response of a first-order loop. By relating T_{loop} to T_{up} using data from the time management scheme shown in Figure A-1, Equation (A-3) may be rewritten as

$$B_L = \ln(.05) / \left(-4\left(\frac{T_{up} - T_{data}}{4} - T_s\right)\right) . \qquad \text{Eq. (A-4)}$$

If T_{data} and T_s are held constant, the minimum B_L will decrease as T_{up} increases. Therefore, as T_{up} increases, σ_c will decrease. While receiver accuracy is of primary concern when choosing T_{up}, there are several other factors which should be considered.

The first of these factors is the amount of time required for the receiver to collect the data being transmitted by each satellite being tracked. Without exploring the details of the format of the satellite transmitted data, 50 update periods are required to collect all the data from a single satellite using the time management scheme shown in Figure A-1. Since all the data from a spare satellite must be collected prior to using it as an active satellite in the navigation solution, the update period should be kept short so as to allow rapid incorporation of a spare satellite as an active satellite.

Another factor which needs to be considered is the magnitude of the code loop prepositioning error. In order for Equation (A-1) to hold true, the prepositioning error must be less than the capture range of the code tracking loop and the residual error must be insignificant when compared to σ_c. (Recall that the code tracking loop is designed to leave a residual error of less than 5 percent of the prepositioning error).

The function of the prepositioning algorithm is to predict the pseudorange to any given satellite and therefore the position in time of the signal from that satellite at the beginning of the next dwell period for the satellite. For a code tracking loop with a capture range of plus or minus one half a code chip (489 nsec), the prepositioning algorithm must be accurate to plus or minus 147 meters. If the prepositioning algorithm operates by projecting the past rate of change of the pseudorange (range rate) forward to determine the new pseudorange at a future time, the maximum prepositioning error (E_p) can be shown to be

$$E_P = E_{rr}(T_{up} - T_{dwell}) + 1/2(a_{sat}(\theta) + a_{vessel} \cos\theta)(T_{up} - T_{dwell})^2 . \qquad \text{Eq. (A-5)}$$

E_{rr} is the range rate measurement error, which can be shown to have a two-sigma value of 0.0103 meters/sec for an algorithm which uses the carrier signal doppler shift to determine range rate. Theta (θ) is the satellite elevation angle, a_{vessel} is the vessel acceleration, and $a_{sat}(\theta)$ is the pseudorange acceleration due to satellite motion as a function of elevation angle. For a vessel accelerating at 0.03 G's, the maximum prepositioning error can be shown to be

$$E_p = .0103\,(T_{up} - T_{dwell}) + .178\,(T_{up} - T_{dwell})^2 \text{ meters}. \qquad \text{Eq. (A-6)}$$

When using a reasonable update period, both the prepositioning error and the residual error are within acceptable limits.

The final and perhaps most important additional factor that should be considered in selecting an update rate is the position update rate required by the user. The maneuvering characteristics of the target user's vessel, the rate at which a user can assimilate position information, and other such factors should all be considered. Based upon the above factors, an update period of 5.4 seconds was chosen for use during the remainder of the study.

APPENDIX B. POSITION CALCULATION

This appendix describes an algorithm to calculate a user's position and clock error from sequential pseudorange measurements. The position calculated is the user's position at the time at which the final pseudorange measurement was taken. The algorithm utilizes three measured pseudoranges (P_1, P_2, P_3), and an assumed user distance from the center of the earth (R). In this case, R is assumed to be constant. However, based upon the assumed user position prior to calculating its position, the WGS-72 geoid should be incorporated to increase the accuracy of the solution. All coordinates are earth centered earth fixed cartesian coordinates.

Prior to calculating the user's position, the processor has access to the following variables which are based upon past measurements of user position and clock error and on satellite position data received from each satellite.

X_n, Y_n, Z_n: The position of n^{th} satellite at the time that it transmitted the signal measured by the user.

$\dot{\bar{X}}$, $\dot{\bar{Y}}$, $\dot{\bar{Z}}$: The user's assumed velocity in each of the three coordinates.

$\dot{\bar{T}}$: The user's clock drift rate in meters/sec.

ΔT: The time between sequential pseudorange measurements.

R: The assumed user distance from the center of the earth.

The variables for which the algorithm is solving are:

X,Y,Z: The user's position

T: The user's clock error in meters.

The receiver module supplies the position calculator with three pseudoranges which are incorporated into the expressions

$$(X_1-(X-2\Delta T\dot{\bar{X}}))^2 + (Y_1-(Y-2\Delta T\dot{\bar{Y}}))^2 + (Z_1-(Z-2\Delta T\dot{\bar{Z}}))^2 = (P_1-(T-2\Delta T\dot{\bar{T}}))^2, \qquad \text{Eq. (B-1)}$$

$$(X_2(X-\Delta T\dot{\bar{X}}))^2 + (Y_2-(Y-\Delta T\dot{\bar{Y}}))^2 + (Z_2-(Z-\Delta T\dot{\bar{Z}}))^2 = (P_L-(T-\Delta T\dot{\bar{T}}))^2, \quad \text{Eq. (B-2)}$$

$$\text{and } (X_3-X)^2 + (Y_3-Y)^2 + (Z_3-Z)^2 = (P_3-T)^2. \quad \text{Eq. (B-3)}$$

Equation (B-1) incorporates the measurement taken from Satellite 1. Since this measurement was taken $2\Delta T$ before the third measurement was taken, the user's calculated position is adjusted by a factor of $2\Delta TX$, $2\Delta TY$, $2\Delta TZ$ in the equation. Likewise, the user's calculated position is adjusted by a factor of $\Delta T\dot{\bar{X}}$, $\Delta T\dot{\bar{Y}}$, $\Delta T\dot{\bar{Z}}$ in Equation (B-2).

Given the fact that the only unknowns in these equations are X, Y, Z and T, the other terms can be consolidated into constant terms as shown in the equations

$$(k_1-X)^2 + (k_2-Y)^2 J+ (k_3-Z)^2 = (k_4-T)^2, \quad \text{Eq. (B-4)}$$

$$(k_5-X)^2 + (k_6-Y)^2 + (k_7-Z)^2 = (k_8-T)^2, \quad \text{Eq. (8-5)}$$

$$\text{and } (k_9-X)^2 + (k_{10}-Y)^2 + (k_{11}-Z)^2 = (k_{12}-T)^2. \quad \text{Eq. (B-6)}$$

In addition, it is known that

$$X^2 + Y^2 + Z^2 = R^2 \quad \text{Eq. (B-7)}$$

If Equation (B-4) through (B-6) are expanded and R^2 is substituted for all occurrences of $X^2+Y^2+Z^2$, and the constants are consolidated, the expressions below are derived:

$$-2(k_1x + k_2Y + k_3Z) = (k_4-T)^2 + k_{13}, \quad \text{Eq. (B-8)}$$

$$-2(k_5X + k_6Y + k_7Z) = (k_8-T)^2 + k_{14}, \quad \text{Eq. (B-9)}$$

$$\text{and } -2(k_9X + k_{10}Y + k_{11}Z) = (k_{12}-T)^{2)} + k_{15}. \quad \text{Eq. (B-10)}$$

There are now three equations with four unknowns. If a value is assumed for T, then based upon the assumed $\overline{T}$, there will be three linear equations with three unknowns, which are easily solvable.

Based upon past measures of T and $\overline{T}$, T is assumed and the equation is solved for X, Y, and Z. The difference between the assumed distance from the center of the earth and the distance of the calculated position from the center of the earth maybe calculated in the expression

$$D = \sqrt{(X^2 + Y^2 + Z^2)} - R. \qquad \text{Eq. (B-11)}$$

If the absolute value of D is less than some threshold value (0.1 meters was used), then the problem is completed and the position and clock error are known. If D is greater than zero, then the solution places the vessel further from the earth's center than initially assumed. Therefore, the estimate of T must be decreased, which has the effect of increasing the measured range to each satellite and decreasing the distance of the vessel from the center of the earth. If D is less than zero, the estimate of T will be increased.

Based upon the new value for T, the value of $\overline{T}$ and the constants, k_4 and k_8 will be recomputed. It was stated above that k_4 equals $P_1 + 2\Delta T\overline{T}$ and k_8 equals $P_2 + \Delta T\overline{T}$. Equations (B-8) through (B-10) may be resolved. This iterative process continues until D is less than the threshold value.

APPENDIX C. GPS RECEIVER NAVIGATION PROCESSOR SIMULATION PROGRAM

This appendix describes the capabilities and operation of the GPS Navigation Simulator Program used for this study. The program simulates the movement of a GPS receiver-equipped ship along a straight trackline, through a turn, and along another straight trackline. The critical outputs to the user are the crosstrack and along-track position error in the navigation processor module's output at the end of each receiver update period.

There are several models which the program uses in generating the data which is fed into the simulated navigation processor. The first model is the ship position model. This model assumes that the earth is a sphere with a radius of 6,378,135 meters. The user specifies the initial ship position, course, and speed. The magnitude and radius of the turn are also specified by the user. The ship is modeled as maintaining its initial course and speed for 100 receiver update periods. The ship then commences a turn to starboard with a constant turn radius. At the completion of the turn, the ship steams along its final course for 50 receiver update periods. The ship's speed is constant throughout the entire simulated run. The antenna position, which is the actual position to which pseudorange measurements are made, can be changed in relation to the ship's center of gravity (CG). The CG is assumed to be at the waterline and the ship's center of rotation is assumed to be in the same spot as its CG. The height of the antenna above the CG, the ship's roll angle, and roll period can all be specified by the user.

The next model is the satellite constellation model. An 18-satellite constellation is used with the satellites grouped into 6 equally-spaced orbits with 3 equally-spaced satellites in each orbit. The orbits are circular with an inclination angle of 55 degrees, a radius of 26,561,135 meters, and a period of 12 hours. The satellites in each orbit have an orbital offset of 40 degrees with respect to the satellites in adjacent orbits. At a system time of zero, Satellite #1 is directly over the intersection of the equator and the prime meridian.

The most critical model used in the simulation program is the receiver model. The model creates pseudoranges from the ship's position and the position of selected satellites. Using the equations presented in Appendix A, the model computes σ_c for each selected satellite. A Gaussian, zero mean, random variable

with a standard deviation of σ_c is generated. A receiver clock error, based upon user specified clock stability, initial clock offset, clock phase noise, and a model of the growth of clock error as a second-order Markov process, is generated and added to the random variable generated earlier. Finally, this sum is added to the true range from the ship to the satellite. The true range is calculated using the ship position model and the satellite constellation model. The resulting pseudorange is passed to the navigation processor module. The pseudorange does not include an allowance for ionospheric bias errors. The process is repeated for each required pseudorange.

The preceeding models are used to generate pseudorange and satellite position information which is fed into the navigation processor module. This module performs two functions. First, it selects the satellites to be used in computing the ship's position, and it computes the ship's position.

The satellite selection algorithm selects three satellites to be used in computing the ship's position. The algorithm first determines which satellites having elevation angles greater than the mask angle of the receiver are within view of the ship. From among these satellites, the algorithm then chooses a set of three for use. The set of satellites selected will be the set that, when considered with a point at the center of the earth, forms the tetrahedron with the largest volume.

The second function of the navigation processor is to compute the ship's position using the pseudoranges and satellite position information provided by the models. The user may elect to have the processor use the position calculation algorithm in Appendix B with no tracker, with a standard alpha/beta tracker, or with a switched alpha/beta tracker; or the user may elect to have the processor use a Kalman filter in computing the user's position. Section 2 of the report describes the operation of both the alpha/beta trackers and the Kalman filter. The user specifies the tracker or filter parameters to be used by the processor. The user may also specify the assumed earth radius to be used by the processor in calculating the ship's position. (As mentioned previously, the processor uses an assumed value for the radius of the earth when using a 3-satellite navigation solution.) The calculated position of the ship at the end of each update period is passed from the navigation processor module to the error analysis module.

The error analysis module compares the calculated ship position with the actual ship position and calculates the crosstrack and along-track horizontal position error at each point. The program then divides the simulation run into four sections: the startup section, which extends from the start of each run to the point 50 update periods into the run; the approach section, which extends from 50 update periods into the run to the point where the ship starts its turn; the turn section; and the recovery section which extends from the end of the ship's turn to the end of the run. The standard deviation and mean of the crosstrack and along-track error are computed for the approach and turn sections of the run. The standard deviation and mean of the crosstrack and along-track errors for the approach leg are summed in an RSS fashion to give a single mean and standard deviation of the error for that leg. A criterion function is computed by summing twice the standard deviation and the mean. This criterion function is used as the measure of the accuracy of the simulated navigation processor module along the approach leg. The mean error for the turn section is computed from the mean of the crosstrack and along-track error and is used as the measure of the acceleration induced bias error created in the navigation processor during the turn leg. The output to the user is in the form of the computed crosstrack and along-track errors for each point in tabular and graphic form as well as the computed means, standard deviations, and the criterion function.

REFERENCES

1. Benedict, T.R., G.W. Bordner, "Synthesis of an Optimal Set of Radar Track While Scan Smoothing Equations," IRE Transactions on Automatic Control, 1962.

2. Sinsky, A.I., "Alpha-Beta Tracking Errors for Orbiting Targets," Bendix Corp., BCD-TN-81-003, June 1981.

3. Rempfer, P., J. Kuhn, L. Stevenson, "Preliminary Analysis, Civil Marine Applications of NAVSTAR GPS," DOT-TSC-CG245-PM-82-22, June 1982.

4. Anderson, B.D.O., J.B. Moore, "Optimal Filtering," Prentice-Hall, Inc., Englewood Cliffs, N.J., 1979.

5. Sutherland, A.A. Jr., A. Gelb, "Application of the Kalman Filter to Aided Inertial Systems," The Analytic Sciences Corporation, TR-134-1, October 1967.

6. Hartman, H.P., "Analysis of a Dithering Loop for PN Code Tracking," IEEE Transactions on Aerospace and Electronic Systems, January 1974.

75 copies